Intracellular Aβ42 activates p53 promoter: a pathway to neurodegeneration in Alzheimer's disease

Yasumasa Ohyagi,*,[1] Hideaki Asahara,* De-Hua Chui,† Yuko Tsuruta,* Nobutaka Sakae,* Katsue Miyoshi,* Takeshi Yamada,* Hitoshi Kikuchi,* Takayuki Taniwaki,* Hiroyuki Murai,* Koji Ikezoe,* Hirokazu Furuya,* Takeshi Kawarabayashi,‡ Mikio Shoji,‡ Frederic Checler,§ Toru Iwaki,‖ Takao Makifuchi,†† Kazuya Takeda,‡‡ Jun-ichi Kira,* and Takeshi Tabira‡‡

*Department of Neurology, ‖Department of Neuropathology, Neurological Institute, Graduate School of Medical Sciences, Kyushu University, Fukuoka, Japan; †Division of Demyelinating Disease and Aging, National Institute of Neuroscience, NCNP, Tokyo, Japan; ‡Department of Neurology, Neuroscience, Biophysiological Science, Graduate School of Medicine and Dentistry, Okayama University, Okayama, Japan; §Institut de Pharmacologie Moleculaire et Cellulaire, Valbonne, France; ††Department of Clinical Research, National Saigata Hospital, Niigata, Japan; and ‡‡National Institute for Longevity Sciences, Aichi, Japan

To read the full text of this article, go to http://www.fasebj.org/cgi/doi/10.1096/fj.04-2637fje; doi: 10.1096/fj.04-2637fje

SPECIFIC AIMS

Alzheimer's disease (AD) is the major cause of dementia; amyloid β-protein (Aβ), especially Aβ42, plays an important role in AD pathology. Our aims are to find a molecular mechanism of p53-dependent apoptosis induced by intracellular Aβ42 and to determine the significance of intracellular Aβ42 and p53 expression in AD pathology.

PRINCIPAL FINDINGS

1. Cytosolic Aβ expression and induction of p53-dependent apoptosis

We made constructs that express Aβ40, Aβ42, or reverse-sequence Aβ42 (rAβ42) in cytosol under a tetracycline (TC) -sensitive promoter. Each Aβ mRNA was transiently expressed in the SKN-SH human neuroblastoma cell line. We found ~6- and ~2-fold elevations of the p53 mRNA level in Aβ42- and Aβ40-transfected cells, respectively; rAβ42 did not have this effect. Aβ42 mRNA levels were elevated from 5 h after transfection, followed by a parallel elevation of p53 mRNA levels. In Aβ42-transfected cells, 2- to 4-fold increases in MDM2, p21 (WAF-1), Bax, and PIG3 mRNAs, targets of p53, were found. Cell viability was reduced to ~20% in Aβ42-transfected cells ($P<0.01$). Addition of actinomycin D (ActD) or a caspase inhibitor (CI), Z-VAD-fmk, inhibited cell death ($P<0.01$); antisense p53 DNA, inhibited cell death; and TUNEL staining showed many positive cells in Aβ42 transfectants. p53 mRNA and protein were increased ~3-fold and ~1.5-fold by Aβ42 respectively in U2OS (p53+/+) but not in Saos2 (p53−/−) cells; viability of Aβ42-transfected U2OS cells decreased to ~60% ($P<0.01$), suggesting p53 dependent apoptosis.

2. Direct binding of Aβ42 to p53 promoter and activation of promoter activity

Aβ is reported to form a β-hairpin shape followed by a helix-turn-helix (HTH) motif, an essential motif of heat shock transcription factors (HSF) and the p53 promoter contains heat shock elements (HSE). A gel mobility shift assay using a 48-mer p53 promoter oligonucleotide (pp53, see **Fig. 1*B***) revealed that Aβ42, but not Aβ40, bound pp53 dose dependently (Fig. 1*A*). The rAβ42 peptide did not bind pp53; but Aβ40 bound pp53 only when incubated overnight (data not shown). Such Aβ42 binding was not found in Oct-1 or EBNA promoter (Fig. 1*A*, left). An excess of cold pp53, but not nonspecific calf thymus DNA, diminished the binding of Aβ42 to labeled pp53, showing sequence specificity (Fig. 1*B*, upper). Further study using the region-specific 40-mer oligonucleotides revealed that oligonucleotides containing the middle 10 nucleotides in HSE (HSE-A, B, C), but not non-HSE-5′ or non-HSE-3′, bound Aβ42; HSE-B showed the most remarkable binding (Fig. 1*B*, lower). We next made biotinylated HSE-B to coprecipitate Aβ42 using streptavidin-conjugated magnetic beads. The collecting efficiency of synthetic Aβ42 by HSE-B magnetic beads was much improved when nuclear extract proteins (NEP), but not BSA, was coincubated (Fig. 1*C*, upper). Aβ40 was not recovered because of its lower affinity (data not shown). Non-HSE-3′ collected no Aβ42 and mutant (MT) HSE collected minimal Aβ42 (Fig. 1*C*, middle). Approximately 10 pg Aβ42 was recovered from 100 μg NEP of Aβ42-

[1] Correspondence: Department of Neurology, Neurological Institute, Graduate School of Medical Sciences, Kyushu University, 3-1-1 Maidashi, Higashi-ku, Fukuoka 812-8582, Japan. E-mail: ohyagi@neuro.med.kyushu-u.ac.jp

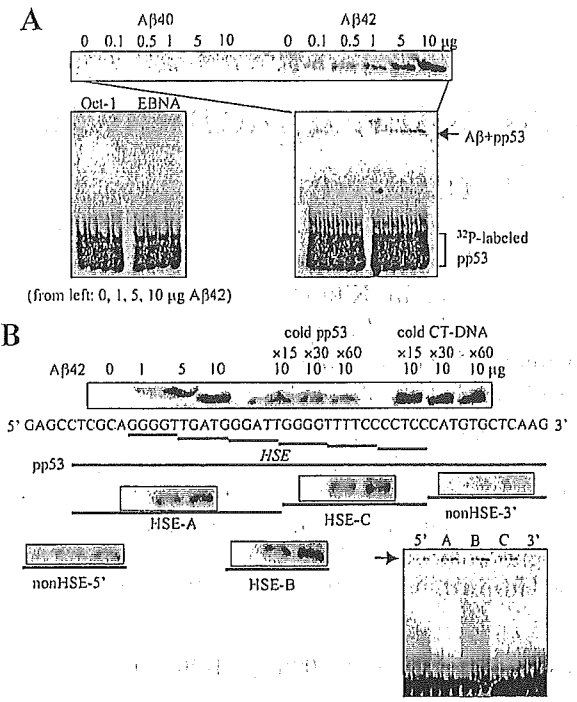

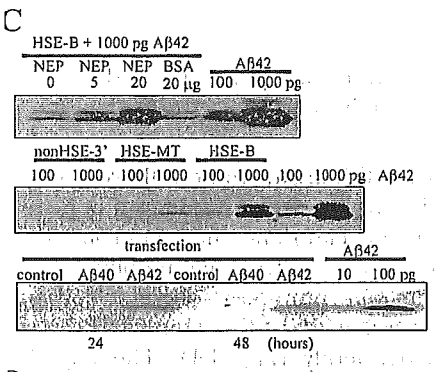

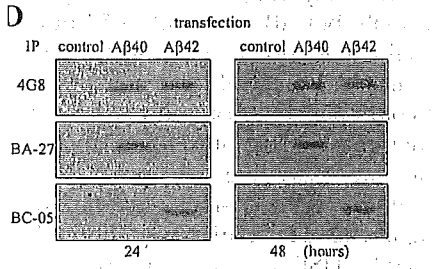

re 1. Gel mobility shift assays of the p53 promoter and and immunoblotting of Aβ collected by magnetic beads. Gel mobility shift assay of synthetic Aβ40 or Aβ42 with led p53 promoter (pp53, right panel) and Oct-1/EBNA panel). *B)* Upper: binding of labeled pp53 and Aβ42 was bited by an excess of cold (unlabeled) pp53 but not by calf thymus (CT) DNA. ×15, ×30, and ×60 = ratios of DNAs to labeled pp53. Lower: binding of labeled region-ific oligonucleotides (bars) and Aβ42. Gel shift images ne bars are isolated from the lower right panel (arrow). *C)* er: immunoblotting detection of Aβ42 (BC-05) collected iotinylated HSE-B and streptavidin-conjugated magnetic ls. Note that addition of NEP, but not BSA, markedly eased the amount of recovered Aβ42. Middle: immuno-ing detection of Aβ42 (BC-05) collected by oligonucleo- (non-HSE-3', HSE-MT, and HSE-B). All samples contained g NEP during incubation. Note that HSE-B recovered Aβ42 h more efficiently than the other two oligonucleotides.

transfected cells (Fig. 1*C*, lower); thus, Aβ42 may bind the p53 promoter in cooperation with other unknown nuclear proteins in vivo and may not form SDS-insoluble fibrils in the nucleus. A further chromatin immunoprecipitation (ChIP) assay showed that the p53 promoter DNA was detected by PCR in eluates recovered from the nuclei of transfected cells by immunoprecipitation with each specific anti-Aβ antibody (Fig. 1*D*). Anti-Aβ40 antibody coprecipitated the p53 promoter; perhaps due to the cross-linking step and PCR detection in the ChIP assay. We made two constructs in which wild-type (WT) or a mutant (MT) pp53 were subcloned upstream of *Firefly* luciferase. The binding affinity of MT pp53 was 50–60% that of WT pp53. Luciferase activity in WT pp53 + Aβ42-coexpressed cells increased ~7-fold; that of MT pp53 + Aβ42-coexpressed cells increased only ~3-fold, which coresponded to lowered binding affinity in vitro. Thus, Aβ42 may directly bind and activate p53 promoter in the nucleus.

3. Oxidative stress-induced cytosolic/nuclear localization of Aβ42 in primary brain cells

To check the biological significance of intracellular Aβ42 on regulating p53 mRNA expression in native neurons, we examined alteration of Aβ42 localization after H_2O_2 treatment. As shown in **Fig. 2***A*, significant cytosolic and partly nuclear accumulation of Aβ42 was observed 6 h after treatment with 1 mM H_2O_2. In association with marked Aβ42 localization (green) in nucleus at 12 h, p53 protein (red) accumulated in these cells. Neurons intensely positive for intranuclear Aβ42 and p53 appeared to be degenerating: dendrites and axons disappeared and the cells became round-shaped (Fig. 2*A*, 12 and 24 h). We earlier found many TUNEL-positive cells in these H_2O_2-treated cultures. Aβ42 became detectable in NEP by immunoblotting at 12 h (Fig. 2*B*), corresponding to marked immunoreactivity in the nucleus at 12 h (Fig. 2*A*). Protein levels of p53 and Bax, a target of p53, began to be elevated 6 h after treatment, but levels of β-actin were not changed (Fig. 2*B*). Similarly, p53 mRNA levels began to be elevated 6 h after treatment (Fig. 2*C*). Thus, Aβ42 may effect on p53 mRNA expression at 6 h, when intranuclear Aβ42 was detectable by immunostaining. The data indicate that oxidative stress may induce Aβ42 accumulation in cytosol, then sequentially in nucleus activating p53 cascade.

4. Intracellular Aβ42 accumulation and p53 expression in degenerating neurons in AD-model mice brain

Intracellular Aβ accumulates with aging from 4 months whereas extracellular Aβ begins to deposit over 10

Lower: immunoblotting detection of endogenous Aβ42 (BC-05) recovered by HSE-B from the NEP of transfected cells. A small amount of Aβ42 is detectable in the NEP of Aβ42-transfected cells. *D)* Chromatin immunoprecipitation (ChIP) assay of p53 promoter DNA using PCR. PCR detected p53 promoter DNA in the eluates immunoprecipitated with 4G8, Aβ40, and 42; BA-27, Aβ40; BC-05, Aβ42.

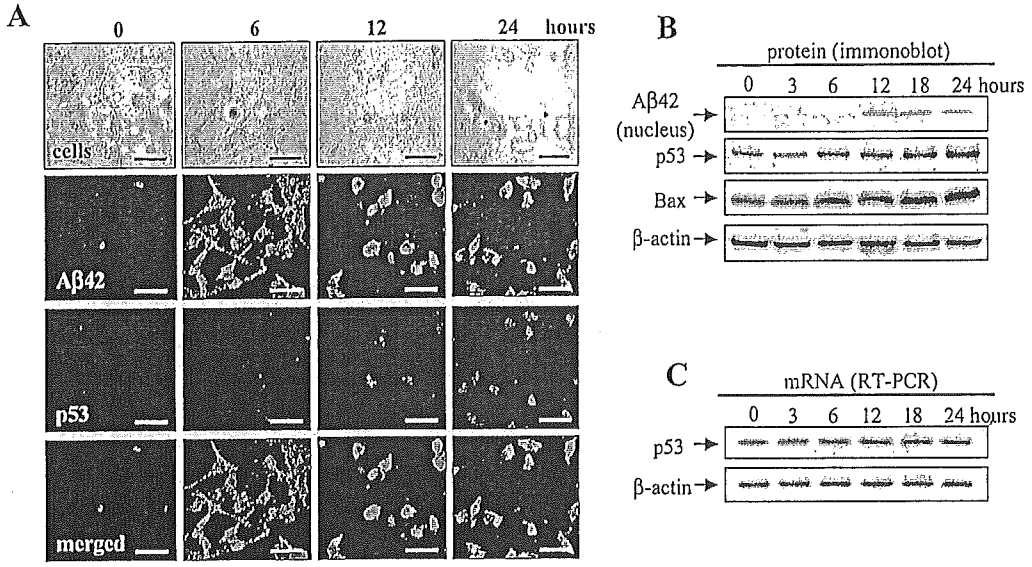

Figure 2. Time course analysis of 1 mM H_2O_2-treated guinea pig primary brain cells. *A)* Double immunostaining of Aβ42 (BC-05, green) and p53 (FL393, red). Aβ42 becomes positive (green) in cytosol and nuclei at 6 h, then localizes to nuclei at 12 h. P53 becomes positive (red) in the whole cell body at 12 h. Scale bars, 20 μm. *B)* Immunoblotting of Aβ42 (BC-05) in NEP and intracellular p53, Bax, and β-actin. *C)* RT-PCR of p53 and β-actin. Consistent with results of immunostaining in panel *A*, p53 mRNA starts to increase at 6 h.

months in Swedish 670/671 mutant APP-Tg mice (Tg2576) brains. However, memory loss in these mice was found to be present at ~6 months of age. In our study, Aβ42 accumulation was found in some degenerating-shaped neurons in 3-, 6-, and 15-month-old mice. Double staining revealed that p53 coincides with intense Aβ42 immunoreactivity in the degenerating-shaped neurons. A similar linkage between intracellular Aβ42 and p53 was found in 17-month-old L286V mutant PS1-Tg mice brains. We checked p53 mRNA levels in 3-month-old APP knockout (APP-KO) mice and these Tg mice brains by semi-quantitative RT-PCR. Similar p53 mRNA levels were found in APP-KO and control mice brains, indicating that Aβ42 may not be obligatory for basic p53 mRNA expression. P53 mRNA expression was stepwise elevated in 17-month-old non-Tg, wild type PS1-Tg and L286V-mutant PS1-Tg mice brains. A similar increase in p53 mRNA was found in Tg2576 in 6- and 10-month-old mice; little was found in 3-month-old mice, indicating that aging may enhance the effect of APP mutation on p53 mRNA expression.

5. Intracellular Aβ42 accumulation and p53 expression in degenerating neurons in AD brain

Immunoblotting indicated that the p53 protein levels in AD frontal cortices were elevated vs. age-matched control brains. Immunocytochemically, intracellular Aβ, but not Aβ40, was observed in many neurons; and neuronal Aβ42 immunoreactivities were sometimes variable. Slightly positive, cytosolic granular-positive, or markedly whole cell body-positive neurons were observed. Remarkably, the markedly whole cell body-positive neurons appeared to be degenerating. Some apoptotic nuclei were TUNEL- and p53-positive. Double immunostaining of p53 and Aβ42 showed some neurons strikingly positive for both antigens in putatively degenerating neurons, similar to Tg mice brains and cultured neurons.

CONCLUSIONS AND SIGNIFICANCE

Our present study suggests a novel biological effect of intracellular Aβ42 as a transcription factor for the p53 promoter. An overload of pathogenic stress as oxidative stress or overproduction of Aβ42 may cause an inappropriate increase in cytosolic and nuclear Aβ42, resulting in enhancement of p53-dependent neuronal apoptosis in AD (**Fig. 3**). Since the ubiquitin-proteasome system is reported to be affected in AD brain, activation of Aβ42 degradation by proteasome may attenuate intracellular Aβ42 pathogenesis. FJ

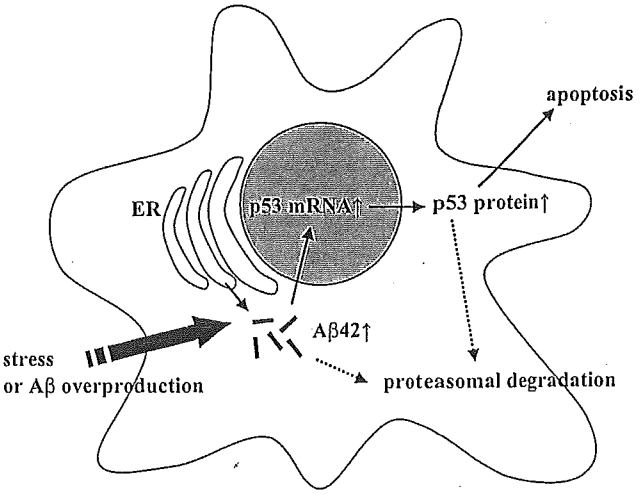

Figure 3. Scheme of intracellular Aβ42 accumulation and p53-dependent apoptosis. Age-related oxidative stress or overproduction of Aβ42 in endoplasmic reticulum (ER) induces Aβ42 accumulation in cytosol. A part of cytosolic Aβ42 may localize to nucleus and activate p53 promoter, enhancing p53-dependent apoptosis. Since p53 protein is degraded by the proteasomal pathway, activation of proteasomal function may attenuate Aβ42 accumulation and p53-dependent apoptosis.

Available online at www.sciencedirect.com
SCIENCE DIRECT®
Biochemical and Biophysical Research Communications 344 (2006) 525–530
BBRC
www.elsevier.com/locate/ybbrc

Altered localization of amyloid precursor protein under endoplasmic reticulum stress

Takashi Kudo [a,*], Masayo Okumura [b], Kazunori Imaizumi [c], Wataru Araki [d], Takashi Morihara [a], Hitoshi Tanimukai [a], Eiichiro Kamagata [a], Nobuhiko Tabuchi [a], Ryo Kimura [a], Daisuke Kanayama [a], Akio Fukumori [a], Shinji Tagami [a], Masayasu Okochi [a], Mikiko Kubo [a], Hisashi Tanii [e], Masaya Tohyama [f], Takeshi Tabira [g], Masatoshi Takeda [a]

[a] *Division of Psychiatry, Course of Internal Medicine, Osaka University Graduate School of Medicine, Osaka, Japan*
[b] *Institute for Oral Science, Matsumoto Dental University, Nagano, Japan*
[c] *Division of Molecular and Cellular Biology, Department of Anatomy, Miyazaki Medical College, Miyazaki, Japan*
[d] *Department of Demyelinating Disease and Aging, National Institute of Neuroscience, Tokyo, Japan*
[e] *Department of Psychiatry, Mie University Graduate School of Medicine, Mie, Japan*
[f] *Department of Anatomy and Neuroscience, Osaka University Graduate School of Medicine, Osaka, Japan*
[g] *National Institute for Longevity Sciences, Aichi, Japan*

Received 9 March 2006
Available online 5 April 2006

Abstract

Recent reports have shown that the endoplasmic reticulum (ER) stress is relevant to the pathogenesis of Alzheimer disease. Following the amyloid cascade hypothesis, we therefore attempted to investigate the effects of ER stress on amyloid-β peptide (Aβ) generation. In this study, we found that ER stress altered the localization of amyloid precursor protein (APP) from late compartments to early compartments of the secretory pathway, and decreased the level of Aβ 40 and Aβ 42 release by β- and γ-cutting. Transient transfection with BiP/GRP78 also caused a shift of APP and a reduction in Aβ secretion. It was revealed that the ER stress response facilitated binding of BiP/GRP78 to APP, thereby causing it to be retained in the early compartments apart from a location suitable for the cleavages of Aβ. These findings suggest that induction of BiP/GRP78 during ER stress may be one of the regulatory mechanisms of Aβ generation.

Keywords: Alzheimer's disease; Endoplasmic reticulum; Amyloid-β peptide; Amyloid precursor protein; BiP/GRP78

The first genetic mutations shown to be involved in Alzheimer disease (AD) were discovered in the amyloid precursor protein (APP) gene. These mutations promote the generation of amyloid-β peptide (Aβ) as a sticky molecule that forms senile plaques in the AD brain. Other AD-causing mutations were subsequently identified in presenilin-1 and -2 (PS1 and PS2, respectively) and shown to enhance the processing of APP into amyloidogenic Aβ. Following these discoveries, many reports have shown that cerebral Aβ accumulation primarily influences the AD brain and subsequent steps in the disease process, including neurofibrillary tangles of tau proteins [1]. Therefore, the amyloid cascade hypothesis has led many researchers to investigate Aβ generation. Recent studies have revealed that APP is first cleaved by a β-secretase, BACE1, at the N-terminus of Aβ, followed by an intramembranous second cleavage at the C-terminus of Aβ by a γ-secretase. The γ-secretase activity is controlled by PS1 complexes consisting of heteromeric molecules, including nicastrin, PEN-2, and APH-1 [2]. Although PS1 is mainly located in the endoplasmic reticulum (ER), γ-complexes have also been identified in the plasma membrane and endosomes where they execute γ-cleavage [3,4].

Recent reports have showed that the endoplasmic reticulum (ER) stress is relevant to the pathogenesis of AD.

* Corresponding author. Fax: +81 6 6879 3059.
E-mail address: kudo@psy.med.osaka-u.ac.jp (T. Kudo).

0006-291X/$ - see front matter © 2006 Elsevier Inc. All rights reserved.
doi:10.1016/j.bbrc.2006.03.173

Nakagawa et al. [5] reported that caspase-12, which causes an ER-mediated apoptosis due to ER stress, contributes to Aβ neurotoxicity. It has been also reported that mutations in PS1 and PS2 perturb ER calcium homeostasis causing ER stress [6]. These findings led us to investigate the relationship between ER stress and Aβ generation, i.e., APP processing. In the present study, we show that ER stress affects APP processing by inducing a molecular chaperone.

Materials and methods

Cell culture and cell lines. SH-SY5Y human neuroblastoma cells were stably transfected with Swedish mutant APP670/671 (SY5Y/swAPP). The appearance and growth rate of SY5Y/swAPP cells were similar to those of mock vector-transfected cells. HEK293 cells were stably transfected with V5-tagged nicastrin (293/Nct-V5). Primary fibroblasts were obtained from PS1/PS2$^{-/-}$ mice embryos on embryonic day 14.5. All cells were cultured in Dulbecco's modified Eagle's medium (DMEM; Gibco, Grand Island, NY, USA), supplemented with either 10% fetal calf serum (FCS) for SH-SY5Y cells or 20% FCS for HEK293 cells and embryonic fibroblasts.

Antibodies. An anti-Aβ42 monoclonal antibody, KM10, was obtained by serial immunization of mice with the synthetic peptide MVGGVVIA. An anti-PS1 antibody was raised against a synthetic peptide corresponding to residues 1–14 of human PS1. An anti-V5 antibody (Invitrogen, Carlsbad, CA, USA) was used for BN-PAGE. An anti-APP antibody (Chemicon, Temecula, CA, USA) was used for immunoblotting. Anti-Aβ antibodies, 4G8 and 6E10 (Signet Pathology Systems Inc., Dedham, MA, USA), were used for immunoprecipitation and immunoblotting of Aβ, respectively. Anti-calnexin and anti-Lys-Asp-Glu-Leu (KDEL) antibodies recognizing BiP/GRP78 (Stressgen, Victoria, BC, Canada) were used for immunoprecipitation and immunoblotting as ER markers. An anti-GM130 antibody (BD Biosciences, Mississauga, ON, Canada) was used for immunoblotting as a *cis*-Golgi marker. An anti-β-actin monoclonal antibody was purchased from Chemicon.

ER stress. At 2 days before stimulation by ER stressors, 3×10^5 SY5Y/swAPP cells were plated in 10-cm diameter dishes, and then given fresh culture medium on the following day. In all ER stress response experiments, we used culture dishes showing 70–80% confluency to avoid stress induced by overgrowth. On the day of stimulation, the cells were placed in fresh medium for at least 60 min before treatment to create similar conditions in each dish. Appropriate doses of thapsigargin and tunicamycin (Sigma, St. Louis, MO, USA) were applied for 24 h as ER stress inducers. Control dishes were treated by simply changing the culture media.

Immunoprecipitation and immunoblotting. Following centrifugation of 10-ml aliquots of SY5Y/swAPP media at 2500*g* for 5 min, 15 μl of protein G–Sepharose (Gibco), 5 μl of 4G8 (anti-Aβ antibody), 10 μl of 1 M Tris–HCl, pH 7.8, 8 μl of 0.5 M EDTA, and 8 μl protease inhibitor cocktail (Sigma) were added to 8 ml of each supernatant. After allowing the immunoreactions to proceed for 18 h, the beads were washed four times with RIPA buffer, boiled with sample buffer for 5 min, and applied to a 15/25 PAG Mini gel (Daiichi, Tokyo, Japan). Following SDS/PAGE, the separated proteins were transferred to a nitrocellulose membrane and probed using 6E10 (anti-Aβ antibody).

ELISA. ELISA kits for Aβ 40 and Aβ 42 were purchased from Biosource International (Camarillo, CA, USA) and used according to the manufacturer's instructions. All ELISAs were carried out in duplicate.

Blue native gel electrophoresis (BN-PAGE). At 1 day prior to analysis, 5–13.5% polyacrylamide gels for BN-PAGE were prepared. Following cell lysis in 1% CHAPSO (Calbiochem, San Diego, CA, USA), 500 mM e-aminocaproic acid, 20 mM Hepes, pH 7.4, 2 mM EDTA, and 10% glycerol, the lysates were incubated on ice for 60 min and then centrifuged at 100,000*g* for 60 min. The supernatants were subjected to BN-PAGE [7]. The gels were subsequently soaked in 0.1% SDS for 10 min and electrotransferred to polyvinylidene difluoride membranes in a standard buffer containing 0.01% SDS.

γ-Secretase assay. Membrane isolation from SY5Y/swAPP cells was carried out as previously described [8]. Briefly, cell lysates were suspended in buffer A (20 mM Hepes, pH 7.5, 50 mM KCl, 2 mM EGTA, and protease inhibitor mixture), homogenized using a Dounce homogenizer, and washed once with buffer A by centrifugation at 800*g* for 10 min. The resulting supernatants were pooled and centrifuged at 100,000*g* for 1 h. The membranes were resuspended in buffer B (20 mM Hepes, pH 7.0, 150 mM KCl, 2 mM EGTA, 1% CHAPSO, and protease inhibitor mixture), solubilized at 4 °C for 1 h, and collected by centrifugation at 100,000*g* for 1 h. For measurement of the γ-secretase activity, the solubilized membranes were incubated at 37 °C in 150 μl of assay buffer (50 mM Tris–HCl, pH 6.8, 2 mM EDTA, and 0.25% CHAPSO) and then incubated with 8 μM of the fluorogenic γ-secretase substrate Nma-GGVVIATVK[DNP]-rrr-NH_2 [8] at 37 °C overnight. After a subsequent incubation with 5 μM of the γ-secretase inhibitor L685,458 (Bachem, Bubendorf, Switzerland) or appropriate doses of thapsigargin or tunicamycin, the reaction mixtures were centrifuged at 16,100*g* for 15 min, transferred to a 96-well plate, and measured in a plate reader using an excitation wavelength of 355 nm and an emission wavelength of 440 nm.

Subcellular fractionation. SY5Y/swAPP cells in 14-cm diameter dishes were harvested in 1.6 ml of ice-cold homogenization buffer (10 mM triethanolamine, 10 mM acetic acid, 250 mM sucrose, 1 mM EDTA, 1 mM DTT, and protease inhibitor cocktail) and homogenized by 10 passages through a 25 G needle. Post-nuclear supernatants were obtained by centrifugation at 9500*g* for 10 min at 4 °C using a Sorvall SS-34 rotor and fractionated by centrifugation in a Nycodenz gradient as described previously [9,10]. Briefly, a step gradient was created in Beckman SW41 centrifuge tubes by loading (from top to bottom) 2.5 ml aliquots of 10%, 14.66%, 19.33%, and 24% Nycodenz solutions in saline buffer. The individual solutions were prepared from a 27.6% Nycodenz stock solution and 0.75% NaCl (both in 10 mM Tris–HCl, pH 7.4, 3 mM KCl, 1 mM EDTA, and 0.02% NaN_3). The tubes were sealed with Parafilm, placed horizontally at room temperature for 45 min and then centrifuged at 37,000 rpm for 4 h at 15 °C using a SW41 rotor to create nonlinear gradients. Next, 800 μl aliquots of the post-nuclear supernatants were layered on top of the gradients and fractionated by centrifugation at 37,000 rpm for 1.5 h at 15 °C. After the centrifugation, 10 fractions (1 ml each) were collected from the top of each tube. The subcellular fractions were characterized by probing with antibodies against specific marker proteins of various subcellular compartments, such as calnexin and GM130.

Incorporation immunoprecipitation. SY5Y/swAPP cells were extracted with 1% Nonidet P-40 lysis buffer, followed by immunoprecipitation using anti-APP antibody 22C11 or anti-KDEL antibody (recognizing BiP/GRP78) and protein G–Sepharose beads. After washing, Western blot analyses were performed with anti-APP or anti-KDEL antibodies.

Transfection with BiP/GRP78. A wild-type hamster BiP/GRP78 expression plasmid was kindly provided by L. Hendershot (St. Jude Children's Research Hospital, Memphis, TN, USA). Hamster BiP/GRP78 shows >99% identity to human BiP/GRP78. SY5Y/swAPP cells were transfected using Lipofectamine 2000 (Invitrogen) according to the manufacturer's instructions.

Statistical analysis. The results are presented as means ± SD. Significant differences among groups were determined using the unpaired Student's *t* test. For all analyses, $p < 0.05$ was considered statistically significant.

Results and discussion

SY5Y/swAPP cells, which were permanently transfected with Swedish mutant APP, at 70–80% confluence were placed in fresh culture medium for more than 60 min before treatment with the ER stressors thapsigargin and tunicamycin at appropriate doses for 24 h. Immunoprecipitation and immunoblotting revealed that thapsigargin treatment decreased the secreted total Aβ in media of SY5Y/swAPP cells in a dose-dependent manner

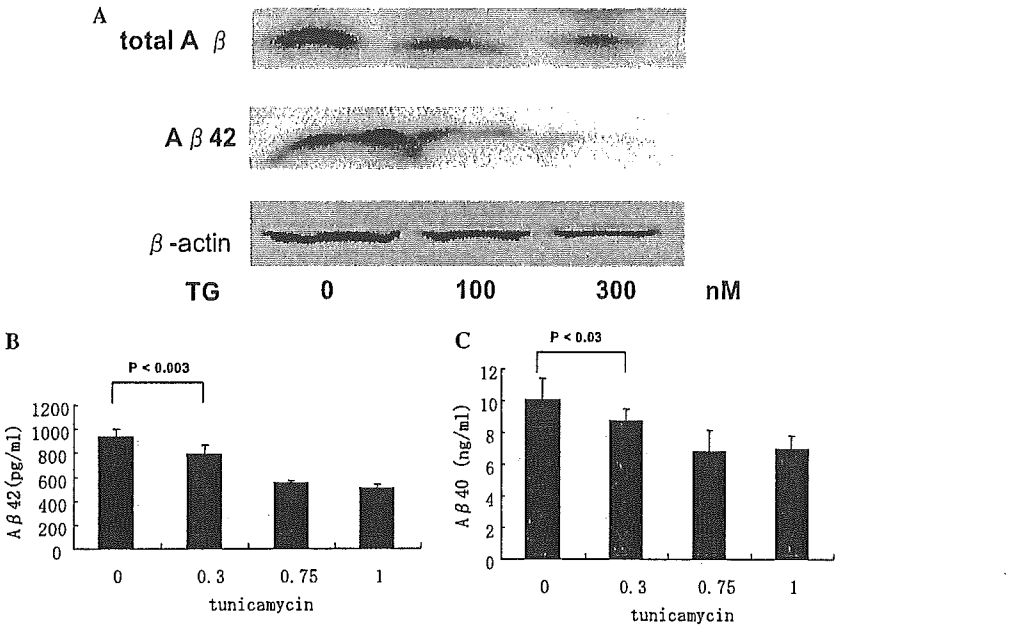

Fig. 1. Reduced Aβ generation following ER stress. (A) SY5Y/swAPP cells were treated with thapsigargin (TG: 0, 100 or 300 nM) for 24 h, and the media were collected and immunoprecipitated with anti-Aβ antibodies (4G8 for total Aβ; KM10 for Aβ 42) and protein G–Sepharose beads. Immunoblotting was probed another Aβ antibody (6E10). (B) The levels of Aβ 42 secreted from SY5Y/swAPP cells treated with 0.3, 0.75 or 1.0 μg/ml tunicamycin were measured by ELISA. Data are expressed as means ± SD ($n = 6$). (C) The levels of Aβ 40 secreted by SY5Y/swAPP cells treated with 0.3, 0.75 or 1.0 μg/ml tunicamycin were measured by ELISA. Data are expressed as means ± SD ($n = 6$).

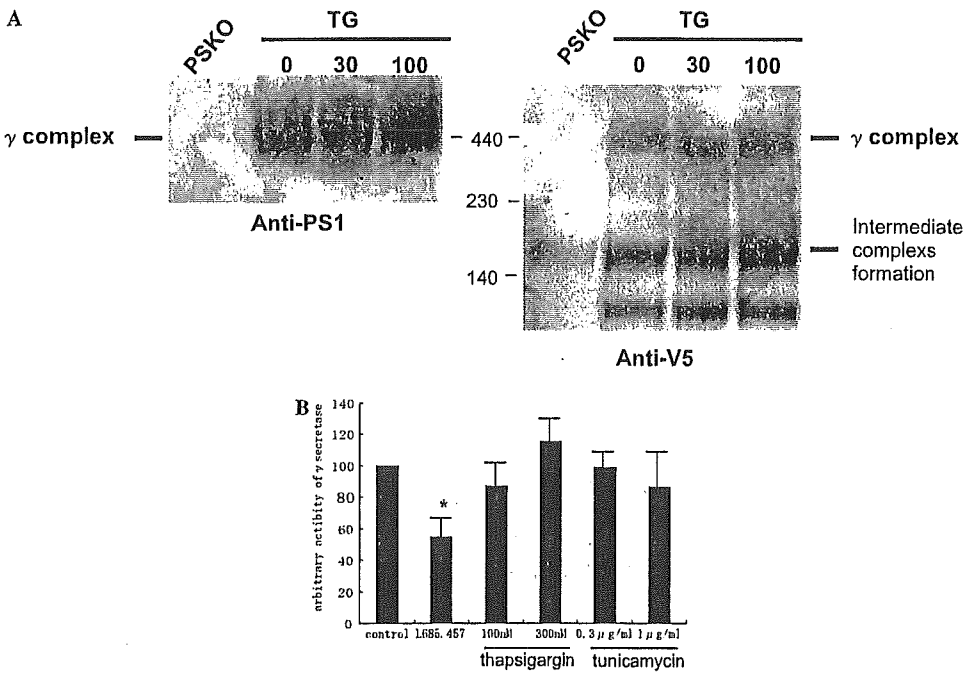

Fig. 2. γ-Secretase activity under ER stress. (A) γ-Complexes under ER stress. 293/Nct-V5 cells treated with thapsigargin (TG) were lysed with 1% CHAPSO, 500 mM e-aminocaproic acid, 20 mM Hepes, pH 7.4, 2 mM EDTA, and 10% glycerol and then centrifuged at 100,000g for 60 min. The supernatants were subjected to BN-PAGE. Immunostaining was probed with anti-PS1 antibodies and anti-V5 antibodies. PSKO: PS1/PS2$^{-/-}$. (B) Solubilized membrane preparations from SY5Y/swAPP cells were incubated with 8 μM of the fluorogenic γ-secretase substrate Nma-GGVVIATVK[DNP]-rrr-NH_2 at 37 °C overnight. After incubation with 5 μM of the γ-secretase inhibitor L685.458 or appropriate doses of thapsigargin or tunicamycin, the reactions were centrifuged at 16,100g for 15 min, transferred to a 96-well plate and measured in a plate reader using an excitation wavelength of 355 nm and an emission wavelength of 440 nm. The values are shown as the percent difference from the control ±SD ($n = 5$). *$p < 0.05$.

(Fig. 1A). The level of Aβ 42 was markedly decreased in the presence of 100 nM thapsigargin (Fig. 1A). The level of intracellular β-actin as an internal control remained unchanged under ER stress, suggesting that these levels of ER stress do not cause apparent cell death. ELISA analyses further demonstrated significant reductions in the Aβ 42 and Aβ 40 levels in media from SY5Y/swAPP cells treated with 0.3, 0.75, and 1.0 μg/ml tunicamycin (Figs. 1B and C). These data suggest that ER stress may suppress Aβ generation.

Recent studies have shown that Aβ generation requires the actions of high molecular mass complexes consisting of PS1, nicastrin, Aph-1, and Pen-2 with γ-secretase activity [11]. 293/Nct-V5 cells, which were transfected with V5-tagged nicastrin, were stressed using appropriate doses of thapsigargin for 24 h, lysed and subjected to BN-PAGE. Immunostaining using anti-PS1 and anti-V5 antibodies revealed that the γ-complexes were unchanged after ER stress (Fig. 2A). Intermediate complexes formation, thought to be immature nicastrin and Aph-1 [12], also remained unchanged after ER stress. Since PS1/PS2$^{-/-}$ mouse (PSKO) embryonic fibroblasts do not have PS1, they do not have any γ-complexes (Fig. 2A). Using a fluorogenic synthetic polypeptide substrate to measure the γ-secretase activity, the doses of the ER stressors thapsigargin and tunicamycin that reduced Aβ production were found to have little influence on the enzyme activity, compared with the conventional γ-secretase inhibitor L685.458 (Fig. 2B). These data indicate that γ-complexes may be assembled and γ-secretase activity may be preserved under ER stress.

Subcellular compartments of SY5Y/swAPP cells were fractionated using a Nycodenz gradient, and each fraction was probed with antibodies against specific marker proteins by immunoblotting analysis. Two distinct subcellular compartments, namely the ER and Golgi, were separated. Fractions 1–5 were designated as belonging to the ER as they possessed calnexin, whereas fractions 8–10 were designated as belonging to the *cis*-Golgi as they showed GM 130 positivity (Fig. 3). Since the bottom fractions from the Nycodenz gradient were assumed to be contaminated with late compartments and plasma membranes, these fractions should contain APP localized in the compartments. Under normal conditions, APP was mainly located in the *cis*-Golgi fractions. Small amounts of APP, especially immature forms, were also distributed in the ER fractions. On the other hand, APP became accumulated in the ER fractions in cells under ER stress in the presence of 1 μM thapsigargin (Fig. 3).

It is assumed that ER stress activates a retrograde transport to the ER from post-ER compartment to avoid the delivery of unfolded proteins. It has been reported that BiP/GRP78, a KDEL protein, binds to unfolded proteins and that a C-terminal KDEL sequence is recognized by the KDEL receptor in post-ER compartments, leading to sorting into COPI vesicles for retrograde transport [13]. Therefore, we hypothesized that APP would bind to BiP/GRP78 under ER stress and undergo retrograde transport. Co-immunoprecipitation experiments using 22C11 and anti-KDEL antibodies revealed that BiP/GRP78 was bound to APP, and that the interaction was prominent under ER stress in the presence of 1 μM thapsigargin. Most of the APP molecules bound to BiP/GRP78 were immature forms, suggesting that BiP/GRP78 is prone to catching immature and unfolded APP (Fig. 4).

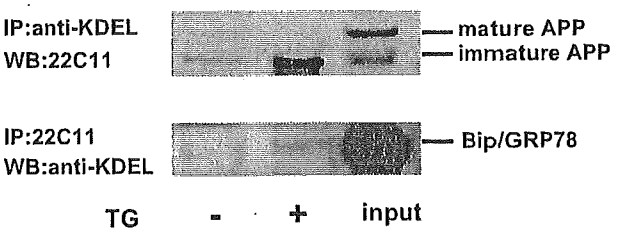

Fig. 4. BiP/GRP78 binding to APP under ER stress. SY5Y/swAPP cells treated with 1 μM thapsigargin (TG) for 24 h were extracted with 1% Nonidet P-40 lysis buffer for immunoprecipitation (IP) with anti-APP or anti-KDEL antibodies (recognizing BiP/GRP78) and protein G–Sepharose beads. After washing, Western blot (WB) analyses were mutually performed with anti-KDEL or anti-APP antibodies.

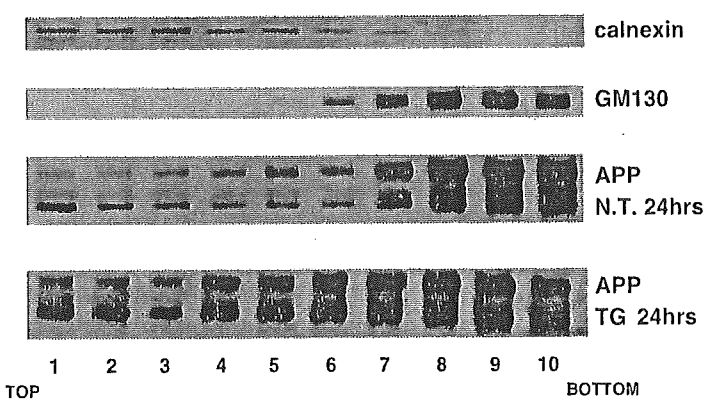

Fig. 3. Shift of APP under ER stress. SY5Y/swAPP cells treated with 1 μM thapsigargin for 24 h or left untreated (non-treated, N.T.) were lysed, fractionated through a Nycodenz gradient, and subjected to Western blot analysis to identify the distributions of calnexin (ER marker), GM130 (Golgi marker), and APP. TG, thapsigargin.

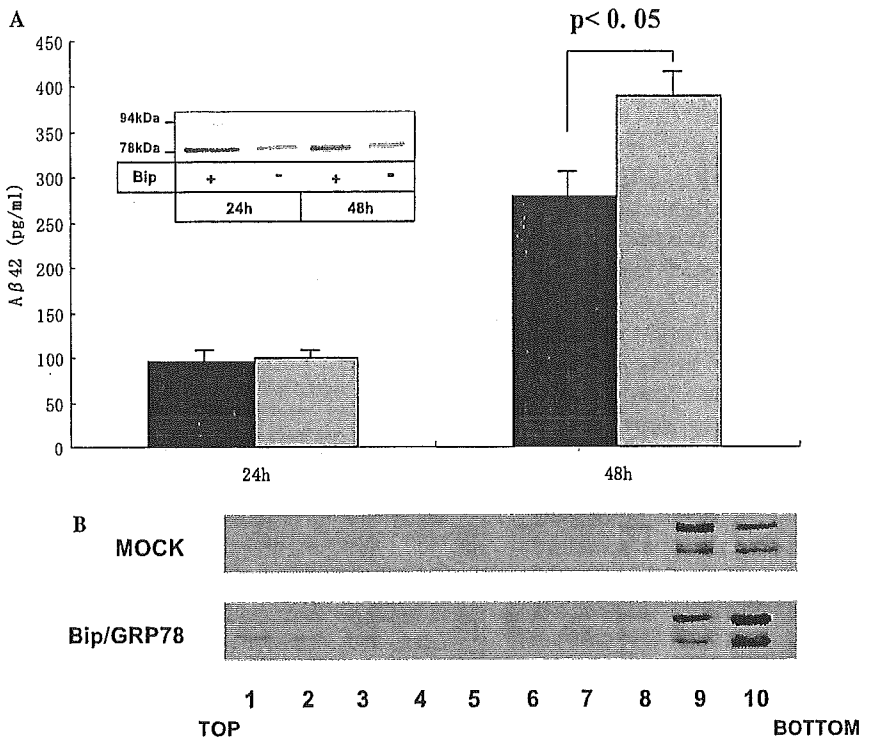

Fig. 5. Reduction in Aβ 42 secretion following transient transfection with a BiP/GRP78 construct. (A) SY5Y/swAPP cells were transiently transfected with a BiP/GRP78 construct and the concentrations of Aβ 42 in the conditioned media at 24 or 72 h after transfection were determined by ELISA. Black bars. BiP/GRP78 transfection; grey bars, mock vector transfection. Inset. Western blotting with an anti-KDEL antibody. Data are expressed as means ± SD ($n = 5$). (B) SY5Y/swAPP cells transfected with a BiP/GRP78 construct or mock vector were lysed, and fractionated through a Nycodenz step gradient.

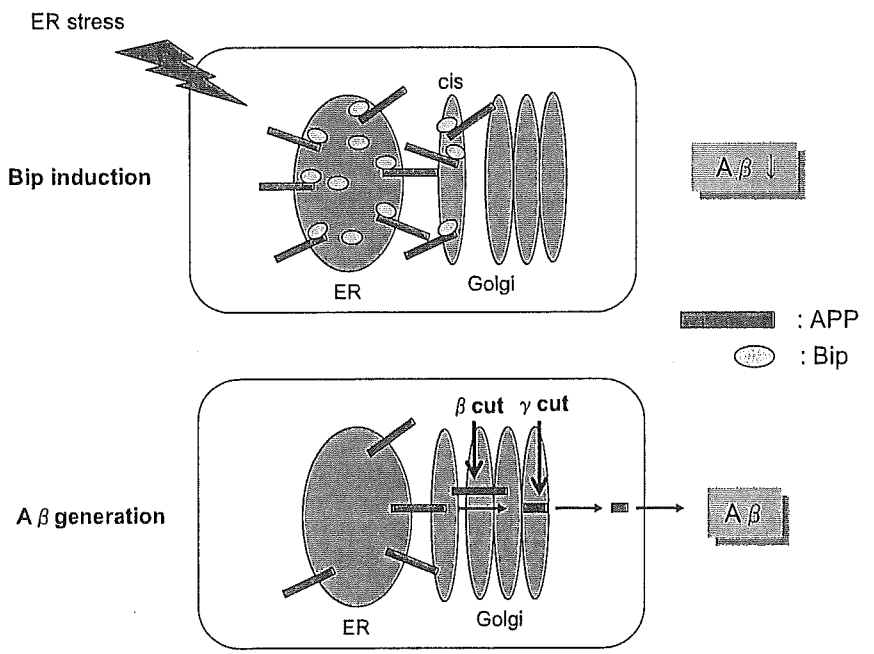

Fig. 6. Altered localization of APP as a result of ER stress. ER stress induces the ER chaperone BiP/GRP78 which binds to APP. APP bound with BiP/GRP78 is retained in the ER because the KDEL sequence of BiP/GRP78 is responsible for its recognition and retrieval from post-ER compartments. Since the β/γ-secretase activity itself is thought to be located in a distal compartment to the ER, ER stress may separate APP from a location suitable for β/γ-secretase cleavage.

To confirm that the induction of BiP/GRP78 reduces Aβ generation, SY5Y/swAPP cells were transiently transfected with a BiP/GRP78 construct. ELISA analysis of Aβ in the conditioned medium demonstrated that the levels of secreted Aβ 40 (not shown) and Aβ 42 were reduced at 78 h after the transfection of BiP/GRP78 (Fig. 5A). Immunoblotting of the Nycodenz gradient fractions of SY5Y/swAPP cells transfected with BiP/GRP78 showed that the induction of BiP/GRP78 caused a shift in APP to the early compartments (Fig. 5B).

These findings suggest that interactions between BiP/GRP78 and immature forms of APP in the ER may prevent APP translocation to distal compartments under ER stress. Regarding the reason why the secretions of Aβ 40 and Aβ 42 were reduced after ER stress, BN-PAGE and γ-secretase assays indicated that the activity of γ-secretase itself may remain unaffected by ER stress. Since γ-secretase activity is thought to exist in the late secretory pathway, plasma membrane, and endosomes [3,4], the APP remaining in the early compartments following ER stress may not reach a location suitable for cutting, resulting in a reduction in Aβ generation (Fig. 6).

IRE1 is one of the transducers for ER stress inducing BiP/GRP78. We previously reported that the maturation of APP was deteriorated in dominant-negative ΔIRE1 cells, a deletion mutant that lacks the kinase and RNase L domains necessary for induction of BiP/GRP78 [14]. Accordingly, we investigated the relationship between ER stress and Aβ generation. The present data indicate that ER stress induces BiP/GRP78 to bind to APP, thereby causing APP to be retained in the early compartments and resulting in a reduction in Aβ generation because β/γ-secretase activity itself is thought to be located in a distal compartment to the ER (Fig. 6). We conclude that the induction of BiP/GRP78 by ER stress may be one of the regulatory mechanisms of Aβ generation. Previously, we also verified that the protein levels of BiP/GRP78 decreased in the brains of sporadic AD as well as familial AD [15]. A combination of these findings and the present data suggest that ER stress may play an important role in AD pathology via the amyloid cascade.

Acknowledgments

This work was supported by a grant from the Ministry of Health, Labor, and Welfare (Mental Health Science), Japan, and a Grant-in-Aid for Scientific Research from the Ministry of Education, Culture, Sports, Science and Technology, Japan.

References

[1] J. Hardy, D.J. Selkoe, The amyloid hypothesis of Alzheimer's disease: progress and problems on the road to therapeutics, Science 297 (2002) 353–356.
[2] C. Haass, Take five BACE and the gamma-secretase quartet conduct Alzheimer's amyloid beta-peptide generation, EMBO J. 23 (2004) 483–488.
[3] P. Cupers, M. Bentahir, K. Craessaerts, I. Orlans, H. Vanderstichele, P. Saftig, B. De Strooper, W. Annaert, The discrepancy between presenilin subcellular localization and gamma-secretase processing of amyloid precursor protein, J. Cell Biol. 154 (2001) 731–740.
[4] W.G. Annaert, L. Levesque, K. Craessaerts, I. Dierinck, G. Snellings, D. Westaway, P.S. George-Hyslop, B. Cordell, P. Fraser, B. De Strooper, Presenilin 1 controls gamma-secretase processing of amyloid precursor protein in pre-golgi compartments of hippocampal neurons, J. Cell Biol. 147 (1999) 277–294.
[5] T. Nakagawa, H. Zhu, N. Morishima, E. Li, J. Xu, B.A. Yankner, J. Yuan, Caspase-12 mediated endoplasmic-reticulum-specific apoptosis and cytotoxicity by amyloid-beta, Nature 403 (2000) 98–103.
[6] M.P. Mattson, S.L. Chan, Dysregulation of cellular calcium homeostasis in Alzheimer's disease: bad genes and bad habits, J. Mol. Neurosci. 17 (2001) 205–224.
[7] H. Schagger, W.A. Cramer, G. von Jagow, Analysis of molecular masses and oligomeric states of protein complexes by blue native electrophoresis and isolation of membrane protein complexes by two-dimensional native electrophoresis, Anal. Biochem. 217 (1994) 220–230.
[8] M.R. Farmery, L.O. Tjernberg, S.E. Pursglove, A. Bergman, B. Winblad, J. Näslund, Partial purification and characterization of γ-secretase from post-mortem human brain, J. Biol. Chem. 278 (2003) 24277–24284.
[9] C. Hammond, A. Helenius, Quality control in the secretory pathway: retention of a misfolded viral membrane glycoprotein involves cycling between the ER, intermediate compartment, and Golgi apparatus, J. Cell Biol. 126 (1994) 41–52.
[10] D. Rickwood, T. Ford, J. Graham, Nycodenz: a new nonionic iodinated gradient medium, Anal. Biochem. 123 (1982) 23–31.
[11] B. De Strooper, Aph-1, Pen-2, and Nicastrin with Presenilin generate an active gamma-Secretase complex, Neuron 38 (2003) 9–12.
[12] M.J. LaVoie, P.C. Fraering, B.L. Ostaszewski, W. Ye, T. Kimberly, M.S. Wolfe, D.J. Selkoe, Assembly of the gamma-secretase complex involves early formation of an intermediate subcomplex of Aph-1 and nicastrin, J. Biol. Chem. 278 (2003) 37213–37222.
[13] K. Yamamoto, R. Fujii, Y. Toyofuku, T. Saito, H. Koseki, V.W. Hsu, T. Aoe, The KDEL receptor mediates a retrieval mechanism that contributes to quality control at the endoplasmic reticulum, EMBO J. 20 (2001) 3082–3091.
[14] N. Sato, K. Imaizumi, T. Manabe, M. Taguchi, J. Hitomi, T. Katayama, T. Yoneda, T. Morihara, Y. Yasuda, T. Takagi, T. Kudo, T. Tsuda, Y. Itoyama, T. Makifuchi, P.E. Fraser, P.St. George-Hyslop, M. Tohyama, Increased production of beta-amyloid and vulnerability to endoplasmic reticulum stress by an aberrant spliced form of presenilin 2, J. Biol. Chem. 276 (2001) 2108–2114.
[15] T. Katayama, K. Imaizumi, N. Sato, K. Miyoshi, T. Kudo, J. Hitomi, T. Morihara, T. Yoneda, F. Gomi, Y. Mori, Y. Nakano, J. Takeda, T. Tsuda, Y. Itoyama, O. Murayama, A. Takashima, P.St. George-Hyslop, M. Takada, M. Tohyama, Presenilin-1 mutations downregulate the signalling pathway of the unfolded-protein response, Nat. Cell Biol. 1 (1999) 479–485.

THE JOURNAL OF BIOLOGICAL CHEMISTRY VOL. 281, NO. 12, pp. 7890–7898, March 24, 2006

Secretion of the Notch-1 Aβ-like Peptide during Notch Signaling*[S]

Received for publication, December 13, 2005, and in revised form, January 23, 2006 Published, JBC Papers in Press, January 23, 2006, DOI 10.1074/jbc.M513250200

Masayasu Okochi[‡1], Akio Fukumori[‡], Jingwei Jiang[‡], Naohiro Itoh[‡§], Ryo Kimura[‡], Harald Steiner[¶], Christian Haass[¶], Shinji Tagami[‡], and Masatoshi Takeda[‡]

From the [‡]Department of Post-Genomics and Diseases, Division of Psychiatry and Behavioral Proteomics, Osaka University Graduate School of Medicine, Osaka 565-0871, Japan, [§]Discovery Research Laboratories, Shionogi and Co., Ltd., Shiga 520-3423, Japan, and [¶]Adolf Butenandt Institute, Department of Biochemistry, Laboratory for Alzheimer and Parkinson's Disease Research, Ludwig-Maximilians University, D-80336 Munich, Germany

The canonical pathway of Notch signaling is mediated by regulated intramembrane proteolysis (RIP). In the pathway, ligand binding results in sequential proteolysis of the Notch receptor, and presenilin (PS)-dependent intramembrane proteolysis at the interface between the membrane and cytosol liberates the Notch-1 intracellular domain (NICD), a transcription modifier. Because the degradation of the Notch-1 transmembrane domain is thought to require an additional cleavage near the middle of the transmembrane domain, extracellular small peptides (Notch-1 Aβ-like peptide (Nβ)) should be produced. Here we showed that Nβ species are indeed secreted during the process of Notch signaling. We identified mainly two distinct molecular species of novel Nβ, Nβ21 and C-terminally elongated Nβ25, which were produced in an ~5:1 ratio. This process is reminiscent of the production of Alzheimer disease-associated Aβ. PS pathogenic mutants increased the production of the longer species of Aβ (Aβ42) from β-amyloid protein precursor. We revealed that several Alzheimer disease mutants also cause a parallel increase in the secretion of the longer form of Nβ. Strikingly, chemicals that modify the Aβ42 level caused parallel changes in the Nβ25 level. These results demonstrated that the characteristics of C-terminal elongation of Nβ and Aβ are almost identical. In addition, because many other type 1 membrane-bound receptors release intracellular domains by PS-dependent intramembrane proteolysis, we suspect that the release of Aβ- or Nβ-like peptides is a common feature of the proteolysis during RIP signaling. We anticipate that this study will open the door to searches for markers of RIP signaling and surrogate markers for Aβ42 production.

Notch signaling is involved in cell differentiation as well as neurodegeneration (1). The canonical pathway for Notch signaling is mediated by regulated intramembrane proteolysis (RIP)[2] (2). In classical signaling, ligand binding to receptors induces downstream intracellular signals, such as Ca^{2+} influx and protein tyrosine phosphorylation. However, RIP signaling is distinct; the receptor is cleaved, liberating an intracellular fragment from the membrane that translocates to the nucleus where it modifies the transcription of target genes (3, 4).

In general, because both the ligand and the receptor for Notch signaling are transmembrane proteins, and signaling occurs only between neighboring cells, a process also called "local cell signaling" (5–7). Thus, although connections between Notch signaling and tumorigenesis have been reported (8, 9), studies to identify secreted molecules that reflect the level of Notch signaling have not been carried out. As a result, the only widely used method for measuring Notch signaling in living cells has been to employ intracellular reporter plasmids (10, 11).

Upon synthesis, the Notch-1 receptor undergoes furin-like cleavage at site (S) 1, forming a heterodimer that is expressed on the plasma membrane with the cleaved fragments (12, 13). The binding of ligands, such as DSL family proteins, at the plasma membrane induces endoproteolysis of Notch-1 by the ADAM/TACE/Kuzbanian family (14–16). This cleavage occurs at S2 within the extracellular juxtamembrane region and results in shedding of the heterodimerized Notch receptor (14–16). The resulting transmembrane fragment, referred to as Notch extracellular truncation, undergoes constitutive presenilin (PS)-dependent intramembrane proteolysis at S3 and S4, which we refer to as "dual-intramembrane proteolysis" (17–19). The S3 cleavage occurs at the interface between the membrane and cytosol, thus determining the N terminus of NICD (17, 18). The presence of the S4 cleavage near the middle of the transmembrane domain (19, 20) and FLAG-tagged Nβ (19) suggests that a putative Notch-1 fragment (Nβ) is produced during the sequential proteolysis of Notch receptors. However, amino acid sequences of these Notch peptides and the composition of their molecular species remain unknown. Moreover, whether they are secreted during Notch signaling has not been determined.

Like Notch receptors, β-amyloid protein precursor (βAPP) undergoes PS-dependent "dual-intramembrane proteolysis" at γ and ε sites (21). γ-Cleavage, which corresponds to S4 cleavage in Notch-1, results in the secretion of Alzheimer disease (AD)-associated Aβ (22), whereas ε-cleavage, corresponding to the S3 cleavage site in Notch-1, releases the βAPP intracellular domain, which has been suggested to regulate transcription

* This work was supported by the "Program for the Promotion of Fundamental Studies in Health Sciences of the National Institute of Biomedical Innovation (05-26)," grants-in-aid for scientific research on priority areas "Advanced Brain Science Project," "KAKENHI" from the Ministry of Education, Culture, Sports, Science, and Technology, and grants-in-aid from the Japanese Ministry of Health, Labor and Welfare in Japan. The costs of publication of this article were defrayed in part by the payment of page charges. This article must therefore be hereby marked "*advertisement*" in accordance with 18 U.S.C. Section 1734 solely to indicate this fact.

[S] The on-line version of this article (available at http://www.jbc.org) contains supplemental Figs. S1–S3, supplemental Table S1, and supplemental Refs. S1 and S2.

[1] To whom correspondence should be addressed: Dept. of Post-Genomics and Diseases, Division of Psychiatry and Behavioral Proteomics, Osaka University Graduate School of Medicine, D3, 2-2 Yamadaoka Suita 565-0871, Japan. Tel.: 81-6-6879-3053; Fax: 81-6-6879-3059; E-mail: mokochi@psy.med.osaka-u.ac.jp.

[2] The abbreviations used are: RIP, regulated intramembrane proteolysis; Aβ, amyloid-β peptide; AD, Alzheimer disease; βAPP, β-amyloid protein precursor; HFIP, 1,1,1,3,3,3-hexafluoro-2-propanol; N1CS, Notch-1 Lin/Notch Repeat CC > SS; NSAIDs, nonsteroidal anti-inflammatory drugs; NICD, Notch-1 intracellular cytoplasmic domains; MS, mass spectroscopy; MALDI-TOF, matrix-assisted laser desorption ionization-time of flight; Nβ, Notch-1 Aβ-like peptide; PS, presenilin; compound W, 3,5-bis(4-nitrophenoxy)benzoic acid; sw, Swedish; WT, wild type; Tricine, *N*-[2-hydroxy-1,1-bis(hydroxymethyl)ethyl]glycine; Bicine, *N*,*N*-bis(2-hydroxyethyl)glycine; CW, Compound W; PMA, phorbol 12-myristate 13-acetate; CHO, Chinese hamster ovary; DAPT, *N*-[*N*-(3,5-difluorophenacetyl)-L-alanyl]-(*S*)-phenylglycine *t*-butyl ester.

(21, 23, 24). In PS-dependent proteolysis, there is some diversity in the specific sites of cleavage (19, 22, 25).[3] This is an important aspect of PS-dependent proteolysis because the pathological molecule Aβ42 is generated by cleavage of βAPP at γ42, a variant of the γ-cleavage site (22). Generally, Aβ42 accounts for ~10% of Aβ production, and most familial AD-associated PS1/2 or βAPP mutants show an increase in Aβ42 production, a peptide that plays an causative role in AD pathology (22). Although Aβ42 induces the formation of senile plaque both in familial and sporadic AD brains, the high degree of Aβ42 aggregation makes it difficult to determine whether Aβ42 generation is enhanced in the pathogenesis of sporadic AD. Therefore, a surrogate marker that precisely reflects the level of Aβ42 generation could be useful.

Elucidation of the mechanism of Aβ42 generation, *i.e.* how the γ-cleavage diversity occurs, is essential because a small change in the precision of γ-cleavage is sufficient to lead to AD pathology. PS-mediated intramembrane proteolysis is known to occur in many other type 1 transmembrane receptors at a site near the cytosolic interface of the transmembrane domains, corresponding to S3/ε cleavage (26, 27). Also, cleavage corresponding to the S4/γ site, which lies in the middle of the transmembrane domain, has been proposed for Notch-1, βAPP, and CD44 (19, 28). Therefore, whether γ-like cleavage occurs in all the substrates or whether there is any diversity among cleavage sites remains unknown. Also, certain chemicals, such as some nonsteroidal anti-inflammatory drugs (NSAIDs), affect the precision of γ-cleavage, increasing or decreasing the generation of Aβ42 (29, 30), but whether this effect is specific to βAPP or is shared by other substrates has not been determined.

To investigate the mechanism of Nβ secretion during Notch signaling, we utilized mouse Notch-1 and its derivatives as substrates. We found that upon ligand binding full-length Notch-1 undergoes endoproteolysis, which transmits Notch signaling and simultaneously secrets untagged Nβ species. These Nβ species shared a common N terminus (derived from S2 cleavage) but had distinct C termini (derived from S4 cleavage). Interestingly, in many cases, when the relative level of pathological Aβ42 was altered by expression of PS mutants or addition of certain chemicals, the relative level of Nβ25, a major species of longer Nβ, changed concomitantly. These results suggested that Nβ is secreted during Notch signaling and that the proteolytic processes determining the C termini of Nβ and Aβ are very similar.

EXPERIMENTAL PROCEDURES

Antibodies and Reagents—The polyclonal antibody 6521 and the rat monoclonal antibody 5E9 were raised against a synthetic peptide (VKSEPVEPPLPSQ) corresponding to the N terminus of Notch extracellular truncation using methods described previously (31). Antibodies 9E10 against the c-Myc epitope, 4G8 against the Aβ peptide, and H114 against the C terminus of Jagged-1 were purchased. Synthetic peptides VKSEPVEPPLPSQLHLMYVAA (Nβ21) and VKSEPVEPPLPSQLHLMYVAAAAFV (Nβ25) were dissolved in Me_2SO or HFIP and stored at −80 °C (32). Upon use, the peptides in HFIP were dried using a SpeedVac and dissolved in the appropriate solution. S2474 was synthesized by Shionogi and Co. Ltd. The γ-secretase inhibitors (L685,458 and DAPT), PMA, NSAIDs (sulindac sulfide, indomethacin, and naproxen), fenofibrate, farnesyl pyrophosphate ammonium salt, geranylgeranyl pyrophosphate ammonium salt, and Compound W (CW), 3,5-bis-(4-nitrophenoxy)benzoic acid were purchased.

cDNA Constructs—The pCS2 vector containing the cDNA for mouse Jagged-1 (kind gift from Dr. Rafael Kopan) (33) and the pTracerCMV containing in the mNotch-1 cDNA were described previously (kind gift from Dr. Jeffrey S. Nye) (34). The cDNAs encoding N1CS (mN1 LNR CC > SS) (kind gift from Dr. Rafael Kopan) (14) and Notch-1, in which the C-terminal 348 residues were replaced with a hexameric Myc tag (17), were cloned into the pcDNA3-hygro(+) vector. *HES-1*-luc (kind gift from Dr. Alain Israel) (10) and pGa981-6 constructs (kind gift from Dr. Georg W. Bornkamm) (11), which contain the firefly luciferase cDNA under control of the *HES-1* promoter and the hexamerized 50-bp EBNA2-response element of the *TP-1* promoter, respectively, were described previously. The pRL-TK construct was obtained from Promega.

Cell Culture and Cell Lines—HEK293 cells stably expressing βAPP sw and either WT or mutant PS1 were generated and cultured (19, 35). CHO cells stably expressing either WT PS1 or PS1 M146L were cultured as described previously (kind gift from Dr. Dennis J. Selkoe) (36). Cells stably expressing βAPP sw, PS derivatives, or both were maintained in media supplemented with 200 μg/ml G418, 200 μg/ml Zeocin, or both. Cells stably expressing Jagged-1, Notch-1, or N1CS were selected with 100 μg/ml hygromycin.

cDNA Transfection and Reporter Assay—To investigate the formation and function of Nβ, we stably transfected HeLa, CHO, or HEK293 cells with Jagged-1, N1CS, and Notch-1 cDNA constructs using Lipofectamine 2000 (Invitrogen). To study the release of Nβ during Notch signaling, HeLa or K293 cells in 8-cm dishes were transiently transfected with 5 μg of plasmids encoding Notch ligands and/or receptors, 5 μg of plasmids encoding the firefly luciferase reporter (*HES-1*-luc or pGa981–6), and 50 ng of the control *Renilla* luciferase reporter plasmid pRL-TK. The next day, the media were replaced, and the cells were lysed with 1× Passive Lysis Buffer (500 μl) (Promega) and freeze-thaw treatment. The pulse-chase experiment to detect the Nβ level was carried out at the same time. Firefly and *Renilla* luciferase activities in the lysates were measured with a dual luciferase reporter assay system (Promega).

Pulse-Chase Experiment—The cells were treated for 2 h with 1 μM L685,458 or 1 μM DAPT to inhibit γ-secretase activity or 20 ng/ml PMA to increase the efficiency of S2 cleavage. Next, following starvation in methionine-free minimum Eagle's medium, the cells were metabolically labeled overnight with 450 μCi of [^{35}S]methionine/cysteine (Redivue Promix; Amersham Biosciences) containing 5% dialyzed (*i.e.* amino acid-free) fetal calf serum and γ-secretase inhibitors or PMA. NSAIDs, compound W, fenofibrate, farnesyl pyrophosphate ammonium salt, and geranylgeranyl pyrophosphate ammonium salt were added to the media throughout the pulse periods.

Immunoprecipitation/Immunoblotting or Immunoprecipitation/Autoradiography—Collected conditioned media were adjusted to 50 mM Tris (from a stock solution of 1 M Tris, pH 7.4), 1:1000 protease inhibitor mixture (Sigma), and 5 mM EDTA (from a stock solution of 500 mM EDTA, pH 8.0). Next, the media were subjected to immunoprecipitation with antibodies 6521 or 4G8 for Nβ and Aβ, respectively (19). For Jagged-1 and Notch-1 derivatives, cell lysates were prepared (37) and analyzed by immunoprecipitation with antibodies H114 and 9E10, respectively (19). Proteins were separated by Tris-glycine (Invitrogen), Tris-Tricine (Invitrogen), or Tris-Bicine SDS-PAGE as described previously (38). The gels were fixed in 50% methanol, 10% acetic acid or 50% methanol, 5% glutaraldehyde (for Nβ). For immunoblotting, proteins were electrophoretically transferred to a polyvinylidene difluoride membrane and probed with the indicated antibodies (39). For autoradiography, the gels were dried and analyzed by fluorography (19).

[3] S. Tagami, A. Fukumori, and M. Okochi, manuscript in preparation.

Immunoprecipitation/MALDI-TOF MS—Immunoprecipitation followed by MALDI-TOF MS analysis was carried out as described previously (19). Briefly, cell lines were grown to confluence in 8-cm dishes. The culture media were replaced with media with or without 20 ng/ml PMA. After 6 h, the media were collected and immunoprecipitated by incubation for 8 h at 4 °C with antibody 6521. Following washing, immunoprecipitated peptides were eluted and analyzed by MALDI-TOF MS. Molecular masses and heights of the MS peaks were calibrated with angiotensin (Sigma), bovine insulin β-chain (Sigma), or both.

RESULTS

Notch-1 Peptides Are Secreted Extracellularly during Notch Signaling—Notch ligand binding to Notch receptors results in sequential proteolysis of the receptor, and PS-dependent intramembrane proteolysis at the interface between the membrane and cytosol (S3) liberates NICD that modifies the transcription of target genes (1) (Fig. 1*A*). Although it was shown that degradation of Notch-1 transmembrane domain requires additional proteolysis near the middle of the transmembrane domain (S4, dual cleavage) (19), secretion of extracellular small peptides (Notch-1 Aβ-like peptide; Nβ) during Notch signaling has not been determined (Fig. 1*A*). Therefore, we first examined whether sequential endoproteolysis of Notch receptors induced upon binding of Notch ligands (1) results in the secretion of Notch peptides. The full-length Notch-1 receptor does not undergo sequential endoproteolysis in the absence of ligand binding, because the S2 cleavage site is masked in the Notch-1 heterodimer formed by S1-cleaved Notch-1 fragments (1). In contrast, Notch-1 LNR CC > SS (N1CS) (Fig. 1*B*) inhibits heterodimerization of S1-cleaved Notch-1 (14). Thus, we expect that N1CS shows constitutive consecutive S1, S2, S3, and S4 cleavage of Notch-1 that usually occurs depending on ligand binding (Fig. 1*B* and supplemental Fig. 1*A*).

To determine whether Notch-1 peptides are secreted, we metabolically labeled HEK293 cells stably expressing Notch-1 or N1CS with [^{35}S]methionine and then performed immunoprecipitation using antibody 6521, which binds to an epitope downstream of S2 (Fig. 1*B*). Most strikingly, autoradiography shows that N1CS-expressing cells secrete Notch-1 peptides of ~3 and 6 kDa, although they were present in different amounts (Fig. 1, *C*, *upper* and *lower panels*, and *D*). The Notch-1-expressing cells, however, produced only trace amounts of these peptides (Fig. 1*C*, *upper panel*). Moreover, addition of PMA to enhance the cleavage at S2 by matrix metalloproteases increased the level of released Notch-1 peptides by 4.73 ± 0.01-fold (Fig. 1, *C* and *D*). On the other hand, addition of γ-secretase inhibitors (L685,458 or DAPT) to inhibit dual-intramembrane proteolysis at S3 and S4 by PS-dependent endoproteolysis greatly reduced the amount of secreted Notch-1 peptide (Fig. 1*D* and supplemental Fig. 1*B*). These results indicated that the Notch-1 peptides are secreted in conjunction with the sequential proteolysis of the Notch-1 receptor and that the production of the Notch-1 peptides is associated with the efficiency of cleavage at S2 and S3/S4 by metalloproteases and PS-dependent proteases, respectively.

We next investigated whether the Notch-1 peptides are secreted during Notch signaling (Fig. 1*E*). Instead of N1CS, we used Notch-1 without any extracellular truncation and mutations (Fig. 1*B*) and observed Notch signaling mediated by Jagged-1 (a Notch ligand). We simultaneously measured the level of Notch signaling and analyzed whether Notch-1 peptides are secreted from cells expressing Jagged-1, Notch-1, or both (Fig. 1*E*). To determine the level of Notch signaling, we measured luciferase reporter activity in cells expressing *HES-1*-luc (10) (*3rd panel* in Fig. 1*E* and supplemental Fig. 2). We also examined the conditioned media for the presence of secreted Notch-1 peptides, as described in Fig. 1, *C* and *D*. We found that cotransfection with Jagged-1 and Notch-1 greatly increased the reporter activity (*3rd panel* of Fig. 1*E*), indicating substantial enhancement of transcription via the *HES-1* promoter. Most surprisingly, the secretion of Notch-1 peptides was also greatly enhanced in cells expressing both Jagged-1 and Notch-1, but it was hardly detectable in cells expressing either Jagged-1 (data not shown) or Notch-1 alone (Fig. 1*E*, *bottom panel*). These results indicated that the secretion of the Notch-1 peptides and the activation of Notch signaling are greatly increased when both Notch-1 and its ligand, Jagged-1, are present. In summary, sequential proteolysis of Notch-1 occurs upon Jagged-1 binding, leading to the production of not only NICD, which is released from the membrane to the cytosol (supplemental Fig. 1*B*), but also novel Notch-1 peptides that are released extracellularly (depicted in Fig. 1*A*).

Determination of the Amino Acid Sequences of the Notch-1 Peptides Reveals Secretion of Nβ—Next, we determined the amino acid sequences of the Notch-1 peptides secreted during the sequential endoproteolytic process of Notch-1 receptor (Fig. 2). The Notch-1 peptide species secreted by N1CS-expressing cells were immunoprecipitated with the 6521 antibodies, and their molecular masses were analyzed by matrix-assisted laser desorption ionization-time of flight (MALDI-TOF) mass spectroscopy (MS) (Fig. 2*A*). The spectrum of the Notch-1 peptides showed two major peaks with molecular masses of 2306 and 2694 Da. We determined the peptide sequences of these species based on that of the sequence surrounding the epitope for the 6521 antibody. Most strikingly, the Notch-1 peptides were found to be composed of peptides S2 to S4 (Table 1, supplemental Fig. 3, and supplemental Table 1). Finally, amino acid sequences of the Notch-1 peptides were determined by MALDI-TOF/TOF MS analysis (supplemental Fig. 3). Therefore, we found that these Notch-1 peptides correspond to the previously predicted Nβ (19). We named the shorter (2306 Da) and longer (2694 Da) Nβ species Nβ21 and Nβ25, respectively, where the number indicates the peptide length (Table 1).

We next synthesized Nβ21 and Nβ25 and analyzed them by MALDI-TOF MS. We confirmed that each peptide showed a single peak in the MS spectrum corresponding to the predicted molecular mass (Fig. 2*B*). We then examined the characteristics of each peptide on Tris-Tricine SDS-PAGE (Fig. 2*C*). We dissolved these peptides in 1,1,1,3,3,3-hexafluoro-2-propanol (HFIP) to prevent the formation of artificial oligomers (32) or in Me_2SO. In both cases, the migration of synthetic Nβ25 and Nβ21 approximately corresponded to 3- and 6-kDa bands, respectively (Fig. 2*C*, *left* and *middle panels*). These results showed that, unlike Nβ25 (or FLAG-tagged Nβ species (19)), Nβ21 may form an SDS-stable homodimer. Like Aβ, we detected extremely low levels of intracellular Nβ compared with secreted Nβ, but we did not detect higher molecular weight aggregates of secreted Nβ21 or Nβ25 on Tris-Tricine SDS-PAGE (data not shown). Also, the intensity of the ~6-kDa band of a mixture prepared with Nβ21 and Nβ25 species was not affected (Fig. 2*C*, *left panel*), indicating that the two Nβ species do not form a heterodimer. Thus, Nβ21 and Nβ25 are separated well by SDS-PAGE. Most interestingly, the migrations of secreted (Fig. 2*C*, *right panel*) and synthetic Nβ (Fig. 2*C*, *middle panel*) on SDS-PAGE were almost identical. Moreover, upon PS1 L166P mutant expression, the ~3-kDa Nβ band on SDS-PAGE and the MS peak corresponding to Nβ25 were predominantly detected (see Fig. 3, *A* and *C*). These findings indicate that Nβ21 and Nβ25 are the major types of secreted Nβ. Measurement of the radioactivity of the two bands indicated that ~20% as much Nβ25 is secreted from cultured cells as Nβ21 (Fig. 2*D*). Based on these results, it appears that the secreted Nβ species correspond to the

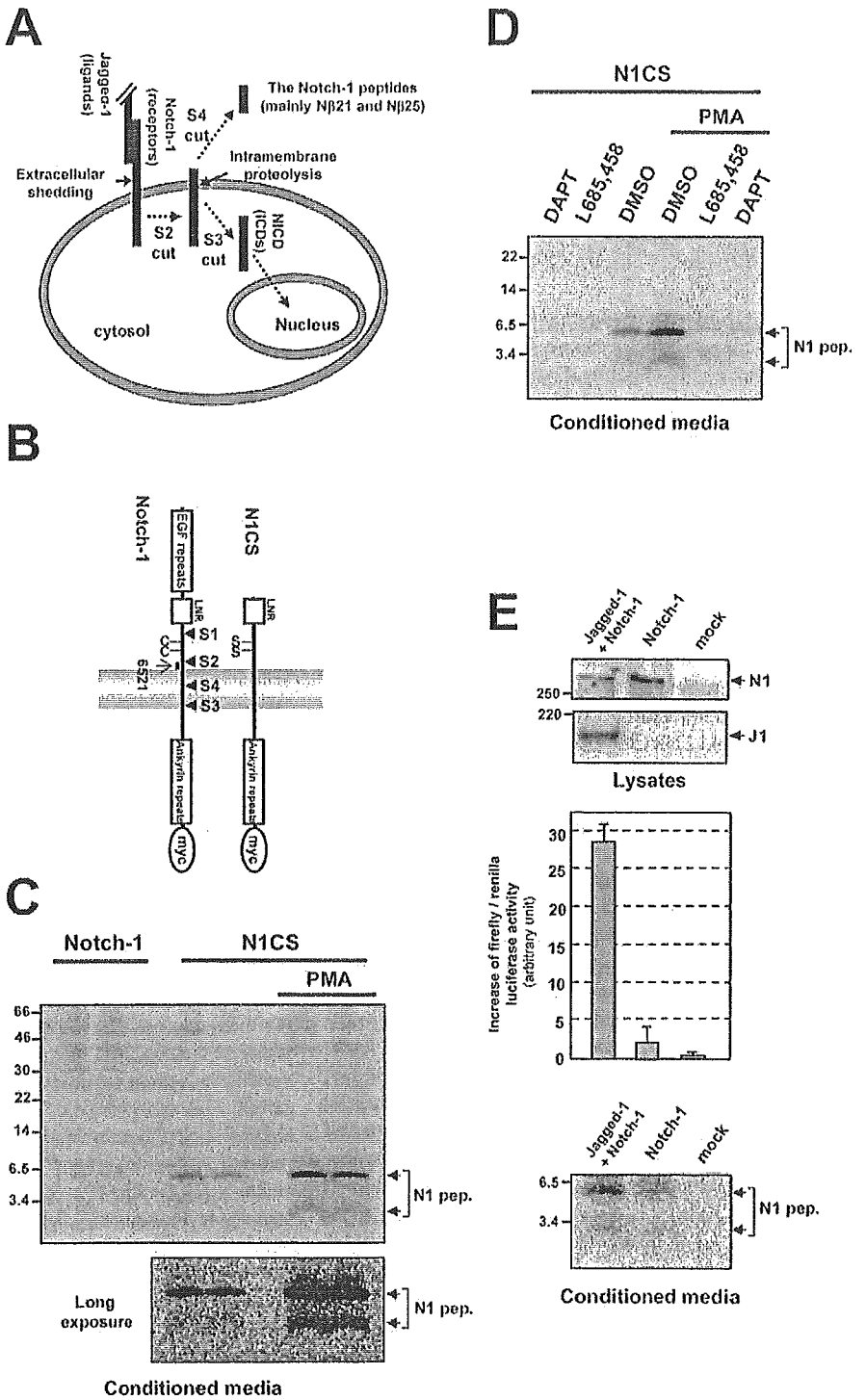

FIGURE 1. **Extracellular release of the Notch-1 peptides by sequential cleavage during Notch signaling.** *A*, schematic representation of the Notch-1 peptide (Nβ) release during canonical Notch signaling. Cleavage of Notch-1 at S4 results in the extracellular secretion of Nβ peptides (see below), whereas cleavage at S3 liberates NICD, which translocates to the nucleus to regulate target gene transcription. *B*, schematic representation of Notch-1 and N1 LNR CC > SS (N1CS), a peptide derived from Notch-1. S1 to S4 and the *gray* zone represent the sites of proteolysis and membrane, respectively. The Notch-1 and N1CS constructs both had C-terminal hexameric Myc tags. Note that the N1CS protein lacks the epidermal growth factor repeats present in Notch-1. Also, to avoid the formation of heterodimers following cleavage at S1, the cysteine residues between S1 and S2 were mutated to serine (14). The *arrow* indicates the recognition site for the 6521 antibody. *C*, immunoprecipitation/autoradiography analysis of Notch-1 peptides in conditioned media from cells treated without or with PMA. Notch-1 or N1CS-expressing cells were labeled by pulse-chase with [^{35}S]methionine. The Notch-1 peptides in conditioned media were separated by Tris-Tricine SDS-PAGE. The *lower panel*, which shows a longer exposure of the autoradiograph, confirms that without PMA treatment the Notch-1 peptides have two distinct molecular weights. Immunoprecipitation/immunoblotting analysis with a 9E10 antibody revealed that the levels of Notch-1 and N1CS expression were similar in the stably transfected cells (data not shown). *D*, immunoprecipitation/autoradiography analysis of conditioned media from N1CS-expressing cells treated with or without γ-secretase inhibitors. The γ-secretase inhibitors DAPT (1 μM) and L685,458 (1 μM) inhibited the secretion of the Notch-1 peptides. Similar results were obtained using HeLa cells expressing N1CS (data not shown). *DMSO*, Me_2SO. *E*, measurement of Notch signaling and the release of Notch-1 peptides in cells transfected with Jagged-1, Notch-1, or both. HEK293 cells were transiently transfected with the indicated constructs along with *HES-1*-luc and the pRL-TK dual luciferase reporter assay system. Empty plasmid vector was used as a mock transfection control. The results show cells expressing *HES-1*-luc. Similar results were obtained using cells expressing pGa981-6 (11) (data not shown). *Top panel*, to confirm the expression of Notch-1, immunoprecipitation/immunoblot analysis was carried out using anti-Myc antibody 9E10. *2nd panel*, Jagged-1 expression was determined using anti-Jagged-1 antibody H114. *3rd panel*, assay of Notch downstream signaling. A dual luciferase reporter assay was performed to compare the transcriptional activity of the *HES-1* promoter in each condition. *HES-1* promoter activity was measured as the relative ratio of firefly and *Renilla* luciferase activities. All values were corrected by the background luciferase activity in endogenous Notch-expressing cells transfected with *HES-1*-luc and pRL-TK. *Bottom panel*, conditioned medium from [^{35}S]methionine-labeled cells was analyzed by immunoprecipitation/autoradiography using antibody 6521.

sequence between S2 and S4 of Notch-1 and that Nβ is made up of two major species, Nβ21 and Nβ25, of which the former is predominant in cell culture (Fig. 2*D*).

Several Familial AD-associated PS1 Mutants Increase the Generation of Elongated Nβ as Well as the Pathological Elongated Aβ—Our results show that intramembrane cleavage of Notch-1 at S4 generates two major Nβ species. We therefore refer to these cleavages as S4-21 and S4-25 for Nβ21 and Nβ25, respectively (Fig. 3*D*). S4-25, the minor type of S4 cleavage, is located four amino acids C-terminal to S4-21, the major S4 cleavage. Like Notch-1, βAPP undergoes PS-dependent intramembrane proteolysis near the middle of the transmembrane domain (γ), resulting in the secretion of Aβ, which accumulates in AD brains (22). Topologically, the γ-cleavage site of βAPP corresponds to the S4 cleavage site of Notch-1 (19). Cleavage at γ42, an alternative form of γ-cleavage, generates Aβ42, which plays a causative role in the pathology of AD; therefore, understanding the mechanism of PS-de-

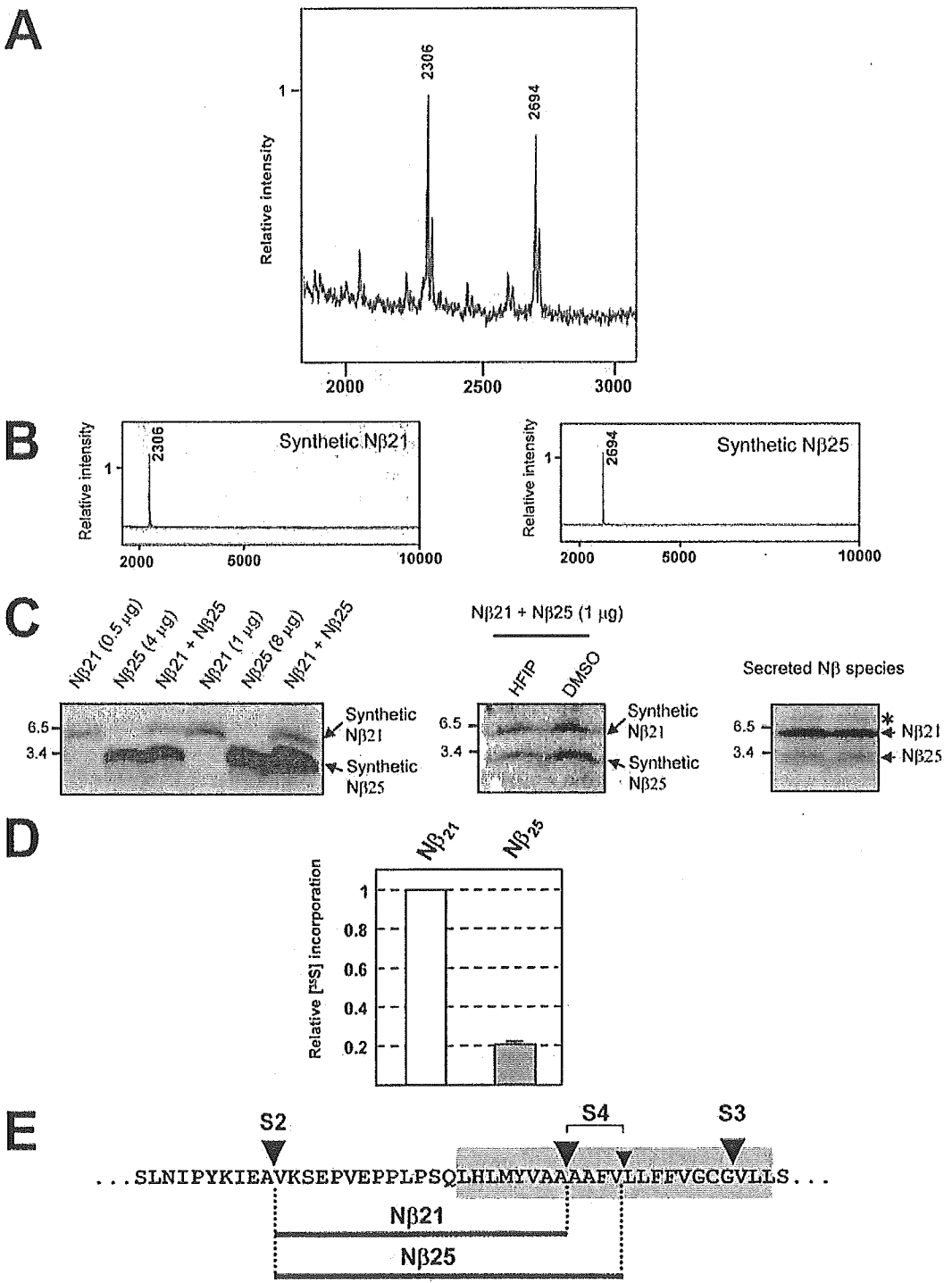

FIGURE 2. **Identification and characterization of secreted Nβ species.** *A*, determination of the molecular masses of the secreted Notch-1 peptides. N1CS-expressing cells were treated with 20 ng/ml PMA for 3 h, and the conditioned medium was analyzed by immunoprecipitation/MS analysis using antibody 6521. Shown is a representative MS spectrum. The MS spectrum was nearly identical for conditioned medium from cells transiently coexpressing Jagged-1 and Notch-1, although the peak heights were lower (data not shown). *B*, MALDI-TOF MS spectra of the synthetic Nβ21 and Nβ25. Although the synthetic Nβ21 appears as an ~6-kDa band on electrophoresis and may form an SDS-stable dimer (*C*), both the synthetic Nβ21 and Nβ25 were identified as single peaks in the MS analysis corresponding to monomeric forms. This shows that the mobility of Nβ21 on SDS-PAGE is lower than predicted for its molecular mass determined by MALDI-TOF MS. *C*, SDS-PAGE analysis of the synthetic Nβ21, synthetic Nβ25, and secreted Notch-1 peptides. *Left panel*, the synthetic Nβ21 and Nβ25 were separated by Tris-Tricine SDS-PAGE and analyzed by immunoblotting with antibody 5E9. *Center panel*, the synthetic Nβ21 and Nβ25 were dissolved in HFIP or Me_2SO and separated by Tris-Tricine SDS-PAGE. Because Aβ tends to aggregate, the synthetic Aβ was suspended in HFIP and then dried to obtain a monomeric Aβ solution (32). Like Aβ, Nβ contains a hydrophobic transmembrane domain sequence; therefore, we suspended the synthetic Nβ in HFIP to completely solubilize the peptides. We then examined whether the mobility on electrophoresis of the Nβ species was affected by the solvents. We were not able to detect the ~3-kDa monomeric Nβ21 band by electrophoresis. Note that similar intensities were observed for the Nβ21 or Nβ25 bands when equal amounts of the synthetic peptides were applied to the gel, indicating that the 5E9 antibody has similar affinities for the Nβ21 and Nβ25. *Right panel*, Nβ peptides in conditioned media from [^{35}S]methionine-labeled cells were separated by Tris-Tricine SDS-PAGE. The *asterisk* indicates a faint ~8-kDa band that was occasionally observed only in conditioned medium. The radioactivity of this band accounts for less than 5% of the total for all Nβ species, indicating a

TABLE 1
Major molecular species of the Notch-1 peptides in conditioned media

M_r (observed)	Peptide	Sequence	M_r (calculated)
2306	Nβ21	VKSEPVEPPLPSQLHLMYVAA	2306
2694	Nβ25	VKSEPVEPPLPSQLHLMYVAAAAFV	2694

pendent intramembrane endoproteolysis is an important issue in AD research (22).

To address the mechanism of cleavage at S4, which results in the production of Nβ, we next tested whether the precision of this cleavage varies simultaneously with the precision of γ-cleavage in βAPP. Most familial AD-associated PS mutants increase the relative level of secreted Aβ42 peptides, although the magnitude of the increase varies between mutants (22). We first tested whether the precision of S4 cleavage was affected by several types of PS mutants. Cells stably expressing the substrates sw mutant βAPP and N1CS, as well as WT or mutant forms PS1 (Fig. 3), were metabolically labeled with [^{35}S]methionine. Secreted Nβ or Aβ species were immunoprecipitated and separated by Tris-Tricine or Tris-Bicine (38) SDS-PAGE, respectively (Fig. 3*A*). To measure the efficiency of Nβ25 generation (S4-25 cleavage), we calculated the relative ratio of radioactivity of the Nβ25 band compared with the total for Nβ bands (including Nβ25; Fig. 3*B*). Using the same samples, we also determined the efficiency of Aβ42 generation (γ42 cleavage). We found that the conditioned medium from cells expressing the PS1 L166P mutant, which has been reported to strongly promote Aβ42 generation (40), had much higher levels of Aβ42 than the medium from cells expressing WT PS1 (Fig. 3, *A*, *lower panel* and *B*). Most strikingly, SDS-PAGE analysis of the Nβ species in the same media (Fig. 3*A*, *upper panel*) showed that the major species was ~3 kDa (Nβ25) and the minor species was ~6 kDa (Nβ21), which is opposite the relative amounts in cells expressing WT PS1. MS analysis of the media of PS1 L166P expressing cells confirmed that the major secreted Nβ species are Nβ21 and Nβ25 with minor other species (Fig. 3*C*).

Therefore, PS1 L166P greatly enhanced not only the production of the long and pathological form of Aβ (Aβ42), but also the production of the longer form of Nβ (Nβ25) (Fig. 3, *A* and *C*). Likewise, the relative ratio of Nβ25 secreted from cells expressing PS1 L286V, PS1 Δ9, and other tested mutants except for C92S (39) increased compared with cells expressing WT PS1 (Fig. 3*B* and data not shown). We therefore suggest that S4-21 and S4-25 cleavage of Notch-1 are γ40- and γ42-like cleavage of βAPP, respectively (Fig. 3*D*).

Modifications of Intramembrane Proteolysis in an Endogenous WT PS Background Have Similar Effects on the Precision of S4 and γ-Cleavages—Recent findings suggest that the relative level of Aβ42 can be changed without mutations in PS or βAPP by using certain chemicals (29, 30). A subset of NSAIDs either increases (29) or decreases (30) the level of Aβ42 generation. Therefore, we finally examined whether, in an endogenous PS background, chemicals can cause parallel changes in the relative levels of Nβ25 and Aβ42. To lower Aβ42, we used sulindac sulfide (100 μM), indomethacin (100 μM) (29), and a newly developed compound, 3,5-bis(4-nitrophenoxy)-benzoic acid, which is called compound W (CW) (100 μM). CW was the most effective of ~100 tested compounds identified in a computer-based structural similarity search for NSAIDs that affect the production of Aβ42. The cells were treated with the compounds and then subjected to metabolic labeling with [^{35}S]methionine. The levels of Aβ/Nβ species were measured as described in Fig. 3. Remarkably, we found that the tested compounds all decreased the relative level of released Nβ25 as well as Aβ42 (Fig. 4, *A*, *left panels*, and *B*). Of these compounds, the most effective, CW, caused a drastic decrease in the level of secreted Nβ25 (Fig. 4*A*, *upper left panel*) and Aβ42 species (Fig. 4*A*, *middle* and *lower left panels*). Next, we examined the effects of S2474 (20 μM), fenofibrate (100 μM), farnesyl pyrophosphate ammonium salt (10 μM), and geranylgeranyl pyrophosphate ammonium salt (10 μM), which are compounds that raise the level of Aβ42 (30). As expected, these compounds all increased the relative level of Aβ42 (Fig. 4, *A*, *right panels*, and *B*). Notably, in all the cases analyzed, the relative level of Nβ25 generation was simultaneously increased (Fig. 4*B*). Naproxen did not modify the relative level of Aβ42 (29) or Nβ25 (Fig. 4, *B* and *C*). A plot of the ratio of Nβ25 to total Nβ *versus* the ratio of Aβ42 to total Aβ (Fig. 4*C*) showed a strong linear correlation (R^2 = 0.98) between the changes in the relative levels of Nβ25 and Aβ42. Moreover, the total level of Aβ and Nβ was not changed by any of the compounds, suggesting that they affect the selectivity but not the activity of cleavage (Fig. 4*A*). These results indicate that, even in cells expressing endogenous PS, the chemicals caused a concomitant change in the relative levels of Nβ25 and Aβ42.

DISCUSSION

In this study, we showed that Nβ species are secreted from cells as a result of sequential Notch-1 proteolysis during Notch signaling. Upon ligand binding, these peptides are likely generated by PS-dependent intramembrane endoproteolysis at S4 after shedding of the extracellular domain (cleavage at S2). Similarly, AD-associated Aβ species are produced by the PS-dependent proteolysis of βAPP (41, 42). Based on these findings, we suspect that cleavage at the middle of the transmembrane domain and extracellular secretion of Aβ-like peptides (*e.g.* Nβ) are a common occurrence in PS-dependent intramembrane proteolysis, even though secretion of such peptides is not included in the current model of RIP signaling.

The human *Notch-1* homologue, *TAN-1*, was isolated as a protein that binds to a mutant β T cell receptor gene formed by chromosomal translocation in human T lymphoblastic leukemia, suggesting that *Notch-1* is involved in tumorigenesis as well as development (8). Moreover, more than 50% of human T lymphoblastic leukemia, including tumors from all major molecular oncogenic subtypes, have activating mutations in Notch-1 (9). Thus, further studies are necessary to determine whether secreted Nβ participates in tumorigenesis or has any other physiological functions in development. In addition, it will be interesting to investigate whether the amount of secreted Nβ reflects the level of Notch signaling so that Nβ might be used as a tumor marker.

In this study, Nβ consisted mainly of a major Nβ21 species and a minor Nβ25 species, indicating that S4 cleavage occurs primarily at two sites, S4-21 and S4-25, in the middle of the Notch-1 transmembrane domain. This confirms that dual-intramembrane proteolysis occurs at S3 and S4 upon degradation of the transmembrane domain of Notch-1 (19). Moreover, this diversity in the sites of cleavage in the middle of the transmembrane domain is reminiscent of the mechanism producing Aβ42, a peptide that plays a causative role in AD (22). Therefore, we

very minor species of Nβ may be released in addition to Nβ21 and Nβ25. *D*, the relative ratio of Nβ25 to that of Nβ21 in the conditioned media of cells stably expressing N1CS. Cells were labeled with [^{35}S]methionine, and radiolabeled Nβ peptides in the conditioned medium were separated by Tris-Tricine SDS-PAGE. The radioactivity incorporated into each band was measured by fluorography using a STORM 820 (Amersham Biosciences). The radioactivity was normalized by that of the Nβ21 band. The *bars* represent the means of three independent measurements, and the *error bars* indicate the S.D. *E*, schematic representation of two different Nβ species and the S2, S3, S4 in Notch-1. The *gray box* indicates the putative transmembrane domain of murine Notch-1.

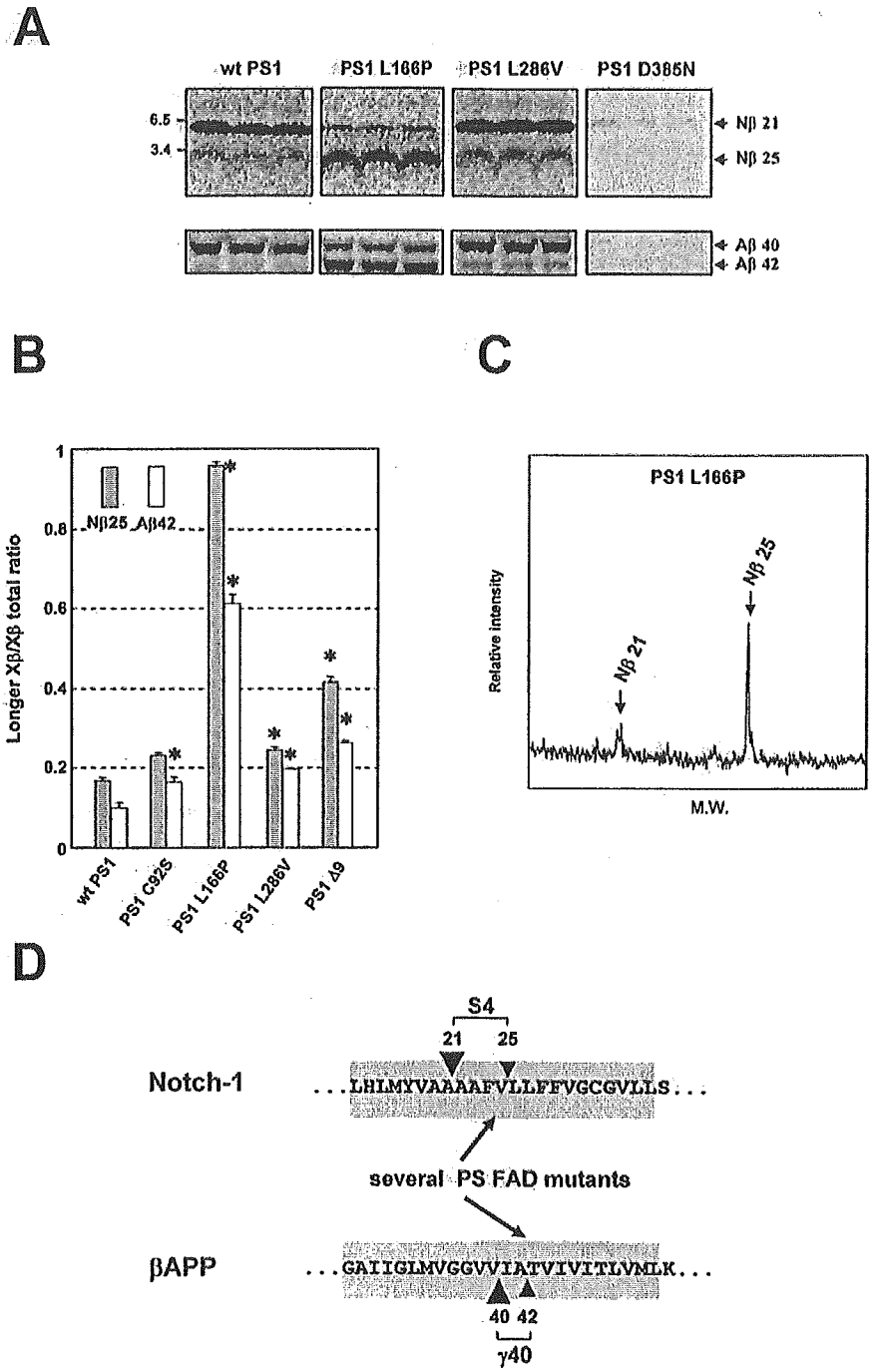

FIGURE 3. **The effects of PS1 mutants on the secretion of the longer Nβ.** *A*, Nβ and Aβ secreted from cells expressing PS1 mutants. *Upper panels*, Nβ species were analyzed as described in Figs. 1 and 2. *Lower panels*, Aβ was immunoprecipitated with antibody 4G8 and separated by Tris-Bicine SDS-PAGE. Note that Nβ and Aβ are hardly detectable in cells stably expressing PS1 D385N, which is dominant negative for PS-dependent protease activity. *B*, the relative ratio of longer Xβ (Nβ25 and Aβ42) secreted by cells expressing familial AD-associated PS mutants. Three independent experiments were carried out with each of two different stable cell lines. *Asterisks* indicate that the ratio of longer Xβ was statistically higher than that in WT PS1-expressing cells ($p < 0.001$ by Student's *t*-test). Similar results were obtained in CHO cells expressing familial AD-associated PS1 mutants (36). *C*, MS spectrum of Nβ species secreted from cells expressing the PS1 L166P mutant. The Nβ25 peak was much higher than the Nβ21 peak comparing the case of WT PS1 (see Fig. 2*A*). Note that the Nβ peptides secreted by the cells are mainly Nβ25 and Nβ21. *D*, schematic representation of the sites cleaved in Notch-1 and βAPP by PS-dependent intramembrane proteolysis during the generation of Xβ species. *Gray boxes* indicate the putative transmembrane domain in Notch-1 and βAPP. The *arrowheads* show the S4 and γ-cleavage sites. *Arrows* show the sites where the efficiency of cleavage is affected by tested familial AD-associated PS mutants.

tested whether the relationship between Nβ21 and Nβ25 was similar to that between Aβ40 and Aβ42. Most familial AD-associated PS mutants increase the generation of Aβ42 (22). Thus, we examined whether the PS mutants result in an extended C terminus in Nβ. We found that, except for the PS1 C92S mutant, the tested PS mutants increased the relative amount of Nβ25. One possible reason for this anomaly is that the mechanism by which the PS1 C92S mutant enhances Aβ42 generation affects Notch-1 processing differently. Another possibility is that the mutant is simply not strong enough to significantly increase the production of Nβ25. Moreover, the PS1 L166P mutants that greatly increased the level of Aβ42 also greatly increased the level of Nβ25. Therefore, in many cases, PS1 mutants that affect the precision of intramembrane proteolysis of βAPP have similar effects on Notch-1 cleavage.

Aβ42 accounts for ~10% of the total Aβ in cells expressing endogenous PS (22). Recently, several NSAIDs were found to either increase or decrease the relative production of Aβ42 (29, 30). This is extremely important because it shows that, as in sporadic AD, the precision of γ-cleavage can change without mutation in either in the substrate (βAPP) or the key enzyme component (PS). This prompted us to investigate whether such compounds also affect the C terminus of Nβ. Because NSAIDs affect the precision of γ-cleavage independently of its

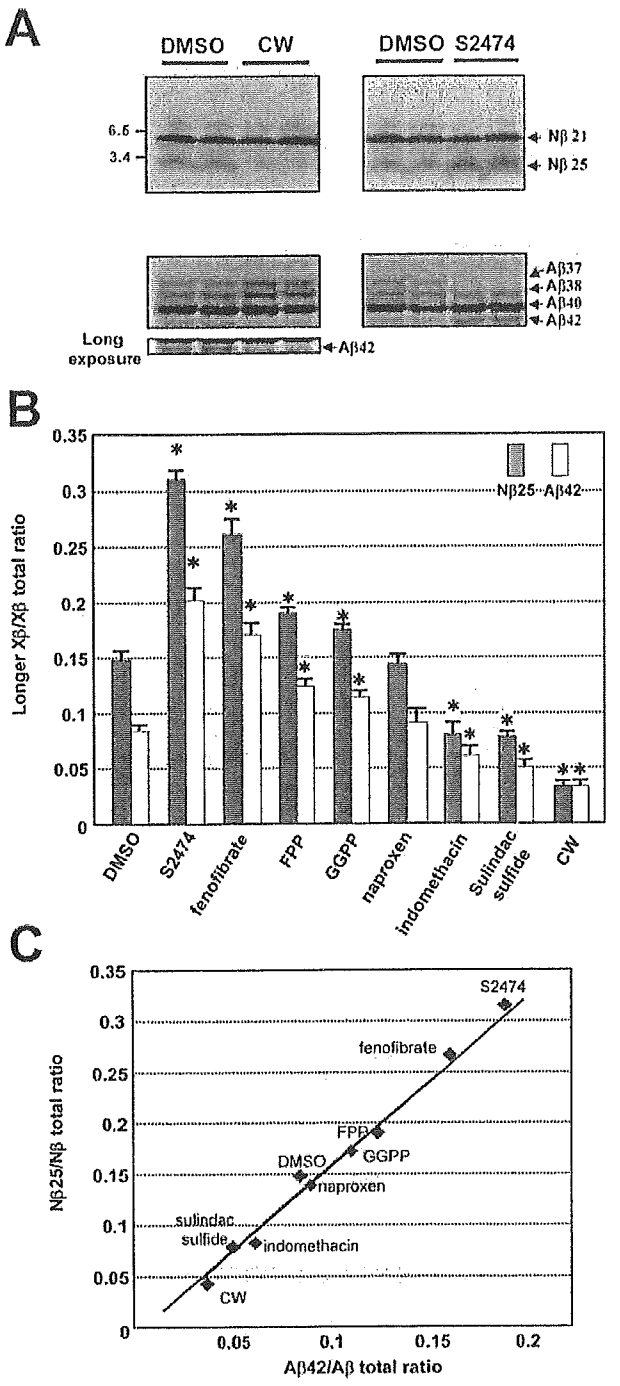

FIGURE 4. **Effects of compounds that modify the generation of Aβ42 on the secretion of longer Nβ25.** *A*, effect of various compounds on the secretion of Nβ and Aβ species from cells expressing βAPP sw and N1CS. Note that the decrease in the level of Aβ42 occurred concomitantly with an increase in the level of Aβ37/38 generation. Likewise, an increase in the level of Aβ42 was accompanied by a decrease in the level of Aβ37/38 generation. *DMSO*, Me_2SO. *B*, the relative ratio of longer Xβ (Nβ25 and Aβ42) secreted from endogenous PS-expressing cells treated with various compounds. *Asterisks* indicate that the relative ratio was statistically different from the Me_2SO control ($p < 0.001$ by Student's *t* test). *C*, a scatter plot of the relative ratio of Nβ25 *versus* the relative ratio of Aβ42. The same experiments as in *panel B* were independently repeated.

anti-inflammatory function (43), we performed a structure similarity search of Aβ42-lowering NSAIDs, and we identified CW as being the most effective of ~100 compounds. Strikingly, all of the tested compounds that affected the level of Aβ42 caused parallel changes in the generation of Nβ25. These results suggest that Nβ25 is the molecular species that corresponds to Aβ42 and that the PS-dependent protease generates longer Nβ and longer Aβ by a common mechanism.

Although increased production of Aβ42 is thought to cause the pathogenesis of most forms of familial AD, abnormalities in Aβ metabolism rather than increased Aβ42 generation are thought to be central to the pathogenesis of sporadic AD (44). Notably, the level of Aβ peptides, especially Aβ42, in peripheral blood and cerebrospinal fluid do not correlate with their levels in the central nervous system because they tend to aggregate. Therefore, whether Aβ42 generation changes in sporadic AD remains unknown. In this study, we showed that longer Aβ-like peptide species (Nβ25) and Aβ (Aβ42) are secreted concomitantly, which suggests that elongated Aβ-like peptides that do not aggregate could be used as surrogate markers for Aβ42 production.

In this study, we found that S4 and γ-cleavages, which occur in the middle of the transmembrane domain, have nearly identical characteristics. Also, S3 and ε cleavages, which occur near the cytosol-membrane interface, are very similar (40, 45).[4] Thus, PS-dependent intramembrane proteolysis may be mediated by a common mechanism in Notch-1 and βAPP. However, the processes mediating cleavage at ε and S3 seem to be distinct from that mediating γ-cleavage (40). Therefore, PS-dependent intramembrane proteolysis in the middle of the transmembrane domain (S4 and γ) and at the membrane-cytosol interface (ε and S3) appears to be mediated by distinct mechanisms.

The effect of NSAIDs on the precision of PS-dependent intramembrane proteolysis was thought to be βAPP-specific because the compounds affected precision of γ-cleavage but not the level of S3 cleavage (which generates NICD) (29). Our results, however, suggest that the effects of the compounds are not substrate-specific but may affect S4- and γ-like cleavages that occur near the middle of the transmembrane domains.

Comparison of the processes and precision of S4 and γ cleavage should help clarify how Aβ and Aβ42, essential molecules in AD pathology, are generated. The βAPP γ-cleavage shares the following characteristics with Notch-1 S4 cleavage. (i) Both of the cleavages occur near the middle of the transmembrane domain (19). (ii) Both have alternative cleavage sites (see Fig. 3*D*). (iii) Several familial AD-associated PS mutations enhance the cleavage efficiencies at minor C-terminal sites of both peptides (S4-25 and γ42). (iv) Several compounds simultaneously change both S4-25 and γ42 cleavage efficiencies. Although the amino acid sequences of the transmembrane domains of Notch-1 and βAPP are quite different, they are thought to both contain α-helical structures (see Fig. 3*D*). Therefore, the common aspects of S4 and γ-cleavage do not appear to be due to similarities in the primary structure of the substrate (transmembrane domains of Notch-1 and βAPP) but rather similarities in the secondary structures or higher structures of the enzyme-substrate complex.

Although there are significant similarities in the two cleavages, there are also some minor differences as follows. (i) The major γ-site is almost in the center of the transmembrane domain of βAPP, whereas the corresponding site in Notch-1, S4-21, is located slightly toward the extracellular side in the transmembrane domain (Fig. 3*D*). (ii) The distance between the major γ40 and the minor γ42 site is two amino acids, whereas the distance between S4-21 and S4-25 is four amino acids (Figs. 2*E* and 3*D*). (iii) The cleavage efficiency at γ42 is ~10%, whereas that of S4-25 is ~20% (Fig. 2*D*). These distinct properties are likely to be at least partly because of differences in the primary structures of the substrates. Comparison of the characteristics of S4 and γ-cleavage should help

[4] A. Fukumori, S. Tagami, and M. Okochi, submitted for publication.

clarify the process of Aβ42 generation; specifically, it appears that the peptide secondary or the higher structure of the enzyme-substrate complex is involved in the efficiency of Aβ42 generation, whereas the primary structure of the substrate transmembrane domain appears to determine the site of the minor cleavage.

When cleaved by PS-dependent intramembrane proteolysis, the βAPP transmembrane domain is thought to maintain an α-helical conformation (46). In this case, the pathological γ42 cleavage would occur in the opposite orientation as the major γ40 cleavage. In contrast, although the corresponding S4-25 site is located more toward the cytosolic side of the transmembrane domain, it is in nearly the same orientation at the S4-21 site. Thus, assuming α-helical structures of the substrate, cleavage at S4-25 and γ42 would be expected to occur by different mechanisms. Because there are so many similarities between the two, we propose that until the cleavage, perhaps in the enzyme-substrate complex, the secondary structures of the substrate transmembrane domains change so that they are no longer α-helices.

In this study we showed that Nβ species (mainly Nβ21 and Nβ25) are released extracellularly during the process of Notch signaling. The Nβ species had identical N termini but different C termini because of diversity in the site of S4 cleavage. Furthermore, the characteristics of the C-terminal elongation of Nβ and Aβ were almost identical. Because many membrane-bound receptors undergo PS-dependent intramembrane proteolysis, we propose that secretion of Aβ-like peptides such as Nβ may be a common phenomenon. This should open the door to a search for the best Aβ-like peptide to serve as a surrogate marker for AD-associated production of Aβ42.

Acknowledgments—We thank Dr. Rafael Kopan, Dr. Jeffrey S. Nye, Dr. Alain Israel, and Dr. Georg W. Bornkamm for providing cDNAs and constructs; Dr. Dennis J. Selkoe for providing cell lines; and Dr. Kazuya Nakao, Dr. Yasuo Ihara, Dr. Maho Morishima, and Dr. Taisuke Tomita for helpful suggestions.

REFERENCES

1. Selkoe, D., and Kopan, R. (2003) *Annu. Rev. Neurosci.* **26**, 565–597
2. Mumm, J. S., and Kopan, R. (2000) *Dev. Biol.* **228**, 151–165
3. Brown, M. S., Ye, J., Rawson, R. B., and Goldstein, J. L. (2000) *Cell* **100**, 391–398
4. Wolfe, M. S., and Kopan, R. (2004) *Science* **305**, 1119–1123
5. Le Borgne, R., Bardin, A., and Schweisguth, F. (2005) *Development (Camb.)* **132**, 1751–1762
6. Schweisguth, F. (2004) *Curr. Biol.* **14**, R129–R138
7. Artavanis-Tsakonas, S., Matsuno, K., and Fortini, M. E. (1995) *Science* **268**, 225–232
8. Ellisen, L. W., Bird, J., West, D. C., Soreng, A. L., Reynolds, T. C., Smith, S. D., and Sklar, J. (1991) *Cell* **66**, 649–661
9. Weng, A. P., Ferrando, A. A., Lee, W., Morris, J. P. T., Silverman, L. B., Sanchez-Irizarry, C., Blacklow, S. C., Look, A. T., and Aster, J. C. (2004) *Science* **306**, 269–271
10. Jarriault, S., Brou, C., Logeat, F., Schroeter, E. H., Kopan, R., and Israel, A. (1995) *Nature* **377**, 355–358
11. Minoguchi, S., Taniguchi, Y., Kato, H., Okazaki, T., Strobl, L. J., Zimber-Strobl, U., Bornkamm, G. W., and Honjo, T. (1997) *Mol. Cell. Biol.* **17**, 2679–2687
12. Blaumueller, C. M., Qi, H., Zagouras, P., and Artavanis-Tsakonas, S. (1997) *Cell* **90**, 281–291
13. Logeat, F., Bessia, C., Brou, C., LeBail, O., Jarriault, S., Seidah, N. G., and Israel, A. (1998) *Proc. Natl. Acad. Sci. U. S. A.* **95**, 8108–8112
14. Mumm, J. S., Schroeter, E. H., Saxena, M. T., Griesemer, A., Tian, X., Pan, D. J., Ray, W. J., and Kopan, R. (2000) *Mol. Cell* **5**, 197–206
15. Brou, C., Logeat, F., Gupta, N., Bessia, C., LeBail, O., Doedens, J. R., Cumano, A., Roux, P., Black, R. A., and Israel, A. (2000) *Mol. Cell* **5**, 207–216
16. Lieber, T., Kidd, S., and Young, M. W. (2002) *Genes Dev.* **16**, 209–221
17. Schroeter, E. H., Kisslinger, J. A., and Kopan, R. (1998) *Nature* **393**, 382–386
18. De Strooper, B., Annaert, W., Cupers, P., Saftig, P., Craessaerts, K., Mumm, J. S., Schroeter, E. H., Schrijvers, V., Wolfe, M. S., Ray, W. J., Goate, A., and Kopan, R. (1999) *Nature* **398**, 518–522
19. Okochi, M., Steiner, H., Fukumori, A., Tanii, H., Tomita, T., Tanaka, T., Iwatsubo, T., Kudo, T., Takeda, M., and Haass, C. (2002) *EMBO J.* **21**, 5408–5416
20. Zhang, J., Ye, W., Wang, R., Wolfe, M. S., Greenberg, B. D., and Selkoe, D. J. (2002) *J. Biol. Chem.* **277**, 15069–15075
21. Haass, C., and Steiner, H. (2002) *Trends Cell Biol.* **12**, 556–562
22. Selkoe, D. J. (2001) *Physiol. Rev.* **81**, 741–766
23. Cao, X., and Sudhof, T. C. (2001) *Science* **293**, 115–120
24. Pardossi-Piquard, R., Petit, A., Kawarai, T., Sunyach, C., Alves da Costa, C., Vincent, B., Ring, S., D'Adamio, L., Shen, J., Muller, U., St George Hyslop, P., and Checler, F. (2005) *Neuron* **46**, 541–554
25. Sato, T., Dohmae, N., Qi, Y., Kakuda, N., Misonou, H., Mitsumori, R., Maruyama, H., Koo, E. H., Haass, C., Takio, K., Morishima-Kawashima, M., Ishiura, S., and Ihara, Y. (2003) *J. Biol. Chem.* **278**, 24294–24301
26. Xia, W., and Wolfe, M. S. (2003) *J. Cell Sci.* **116**, 2839–2844
27. Koo, E. H., and Kopan, R. (2004) *Nat. Med.* **10**, S26–S33
28. Lammich, S., Okochi, M., Takeda, M., Kaether, C., Capell, A., Zimmer, A. K., Edbauer, D., Walter, J., Steiner, H., and Haass, C. (2002) *J. Biol. Chem.* **277**, 44754–44759
29. Weggen, S., Eriksen, J. L., Das, P., Sagi, S. A., Wang, R., Pietrzik, C. U., Findlay, K. A., Smith, T. E., Murphy, M. P., Bulter, T., Kang, D. E., Marquez-Sterling, N., Golde, T. E., and Koo, E. H. (2001) *Nature* **414**, 212–216
30. Kukar, T., Murphy, M. P., Eriksen, J. L., Sagi, S. A., Weggen, S., Smith, T. E., Ladd, T., Khan, M. A., Kache, R., Beard, J., Dodson, M., Merit, S., Ozols, V. V., Anastasiadis, P. Z., Das, P., Fauq, A., Koo, E. H., and Golde, T. E. (2005) *Nat. Med.* **11**, 545–550
31. Okochi, M., Ishii, K., Usami, M., Sahara, N., Kametani, F., Tanaka, K., Fraser, P. E., Ikeda, M., Saunders, A. M., Hendriks, L., Shoji, S. I., Nee, L. E., Martin, J. J., Van Broeckhoven, C., St George-Hyslop, P. H., Roses, A. D., and Mori, H. (1997) *FEBS Lett.* **418**, 162–166
32. Yoshiike, Y., Chui, D. H., Akagi, T., Tanaka, N., and Takashima, A. (2003) *J. Biol. Chem.* **278**, 23648–23655
33. Lindsell, C. E., Shawber, C. J., Boulter, J., and Weinmaster, G. (1995) *Cell* **80**, 909–917
34. Nye, J. S., Kopan, R., and Axel, R. (1994) *Development (Camb.)* **120**, 2421–2430
35. Steiner, H., Romig, H., Grim, M. G., Philipp, U., Pesold, B., Citron, M., Baumeister, R., and Haass, C. (1999) *J. Biol. Chem.* **274**, 7615–7618
36. Xia, W., Zhang, J., Kholodenko, D., Citron, M., Podlisny, M. B., Teplow, D. B., Haass, C., Seubert, P., Koo, E. H., and Selkoe, D. J. (1997) *J. Biol. Chem.* **272**, 7977–7982
37. Okochi, M., Walter, J., Koyama, A., Nakajo, S., Baba, M., Iwatsubo, T., Meijer, L., Kahle, P. J., and Haass, C. (2000) *J. Biol. Chem.* **275**, 390–397
38. Wiltfang, J., Smirnov, A., Schnierstein, B., Kelemen, G., Matthies, U., Klafki, H. W., Staufenbiel, M., Huther, G., Ruther, E., and Kornhuber, J. (1997) *Electrophoresis* **18**, 527–532
39. Okochi, M., Eimer, S., Bottcher, A., Baumeister, R., Romig, H., Walter, J., Capell, A., Steiner, H., and Haass, C. (2000) *J. Biol. Chem.* **275**, 40925–40932
40. Moehlmann, T., Winkler, E., Xia, X., Edbauer, D., Murrell, J., Capell, A., Kaether, C., Zheng, H., Ghetti, B., Haass, C., and Steiner, H. (2002) *Proc. Natl. Acad. Sci. U. S. A.* **99**, 8025–8030
41. De Strooper, B., Saftig, P., Craessaerts, K., Vanderstichele, H., Guhde, G., Annaert, W., Von Figura, K., and Van Leuven, F. (1998) *Nature* **391**, 387–390
42. Wolfe, M. S., Xia, W., Ostaszewski, B. L., Diehl, T. S., Kimberly, W. T., and Selkoe, D. J. (1999) *Nature* **398**, 513–517
43. Sagi, S. A., Weggen, S., Eriksen, J., Golde, T. E., and Koo, E. H. (2003) *J. Biol. Chem.* **278**, 31825–31830
44. Selkoe, D. J., and Schenk, D. (2003) *Annu. Rev. Pharmacol. Toxicol.* **43**, 545–584
45. Chen, F., Gu, Y., Hasegawa, H., Ruan, X., Arawaka, S., Fraser, P., Westaway, D., Mount, H., and St George-Hyslop, P. (2002) *J. Biol. Chem.* **277**, 36521–36526
46. Lichtenthaler, S. F., Wang, R., Grimm, H., Uljon, S. N., Masters, C. L., and Beyreuther, K. (1999) *Proc. Natl. Acad. Sci. U. S. A.* **96**, 3053–3058

Presenilin-Dependent γ-Secretase on Plasma Membrane and Endosomes Is Functionally Distinct†

Akio Fukumori,‡,§ Masayasu Okochi,*,‡,§ Shinji Tagami,‡,§ Jingwei Jiang,§ Naohiro Itoh,§ Taisuke Nakayama,§ Kanta Yanagida,§ Yoshiko Ishizuka-Katsura,§ Takashi Morihara,§ Kojin Kamino,§ Toshihisa Tanaka,§ Takashi Kudo,§ Hisashi Tanii,§ Akiko Ikuta,§ Christian Haass,|| and Masatoshi Takeda§

Division of Psychiatry and Behavioral Proteomics, Department of Post-Genomics and Diseases, Osaka University Graduate School of Medicine, Osaka, Japan, and Adolf Butenandt Institute, Department of Biochemistry, Laboratory for Alzheimer's and Parkinson's Disease Research, Ludwig-Maximilians University, Munich, Germany

Received November 25, 2005; Revised Manuscript Received February 25, 2006

ABSTRACT: The presenilin (PS)/γ-secretase complex, which contains not only PS but also Aph-1, PEN-2, and nicastrin, mediates proteolysis of the transmembrane domain of β-amyloid protein precursor (βAPP). Intramembrane proteolysis occurs at the interface between the membrane and cytosol (ε-site) and near the middle of the transmembrane domain (γ-site), generating the βAPP intracellular domain (AICD) and Alzheimer disease-associated Aβ, respectively. Both cleavage sites exhibit some diversity. Changes in the precision of γ-cleavage, which potentially results in secretion of pathogenic Aβ42, have been intensively studied, while those of ε-cleavage have not. Although a number of PS-associated factors have been identified, it is unclear whether any of them physiologically regulate the precision of cleavage by PS/γ-secretase. Moreover, there is currently no clear evidence of whether PS/γ-secretase function differs according to the subcellular site. Here, we show that endocytosis affects the precision of PS-dependent ε-cleavage in cell culture. Relative production of longer AICDε49 increases on the plasma membrane, whereas that of shorter AICDε51 increases on endosomes; however, this occurs without a concomitant major change in the precision of cleavage at γ-sites. Moreover, very similar changes in the precision of ε-cleavage are induced by alteration of the pH. Our findings demonstrate that the precision of ε-cleavage by PS/γ-secretase changes depending upon the conditions and the subcellular location. These results suggest that the precision of cleavage by the PS/γ-secretase complex may be physiologically regulated by the subcellular location and conditions.

Intramembrane proteolysis by presenilin (PS)/γ-secretase plays a key role in both Alzheimer disease (AD)[1] and regulated intramembrane proteolysis (RIP) signaling (*1*). At least two PS-dependent cleavages occur in the transmembrane domains of substrates such as β-amyloid protein precursor (βAPP), Notch, and CD44 ("dual cleavage"): one near the middle of the transmembrane domain (TM-N) (*2*−*5*) and the other on the border between the transmembrane domain and cytosol (TM-C) (*6*−*10*). The cleavage at the TM-N site of βAPP (γ-cleavage) is essential for Aβ generation and is closely related to AD (*2*, *11*). On the other hand, the cleavage at the TM-C site, including that in Notch-1 (S3-cleavage), generates ICDs (*i*ntracellular *c*ytoplasmic *d*omains) and is involved in RIP signaling (*1*).

In PS-dependent proteolysis, there is some diversity in the specific sites of cleavage (*3*, *5*, *7*−*9*, *11*). A change in cleavage precision can have an important effect on the pathogenesis of AD because Aβ42, a causative factor in AD, is generated by one of the types of γ-cleavage (*2*, *11*). Much time and effort have therefore been dedicated to understanding how the precise site of cleavage is determined. Most familial AD-associated PS and βAPP mutants affect the precision of γ-cleavage (*11*). Because such changes in the precision of γ-cleavage have not been observed in other conditions, it had been generally believed that the precision of this cleavage is not easily changed (*11*). Recent studies, however, have revealed that some chemicals including NSAIDs (*n*onsteroidal *a*nti*i*nflammatory *d*rugs) (*12*, *13*) up- or downregulate pathological Aβ42, indicating that the precision of this cleavage by PS/γ-secretase may change under certain circumstances (*14*). Notably, however, corresponding changes in the precision of ε-cleavage have not been examined.

ICDs including that of βAPP (AICD) and Notch (NICD) are generated by ε- and S3-cleavage at TM-C, respectively (*1*). ICDs are generally involved in translocation of signaling

† This work was supported by the Program for the Promotion of Fundamental Studies in Health Sciences of the National Institute of Biomedical Innovation (05-26), by Grants-in-Aid for Scientific Research on Priority Areas−Advanced Brain Science Project and for KAKENHI from the Ministry of Education, Culture, Sports, Science, and Technology of Japan, and by Grants-in-Aid from the Ministry of Health, Labor, and Welfare of Japan.

* To whom correspondence should be addressed. Tel: 81-6-6879-3053. Fax: 81-6-6879-3059. E-mail: mokochi@psy.med.osaka-u.ac.jp.

‡ Equal contributions.

§ Osaka University Graduate School of Medicine.

|| Ludwig-Maximilians University.

[1] Abbreviations: Aβ, amyloid-β peptide; AD, Alzheimer disease; AICD, βAPP intracellular cytoplasmic domain; βAPP, β-amyloid protein precursor; CMF, crude membrane fraction; CTF, carboxyl-terminal fragment; Dyn-1, dynamin-1; IP-MS, immunoprecipitation−mass spectroscopy; K293, human embryonic kidney 293; PM, plasma membrane; PS, presenilin; sw, Swedish mutant; TM-C, the border between the transmembrane domain and cytosol.

10.1021/bi052412w CCC: $33.50
Published on Web 03/28/2006

molecules to the nucleus to activate target genes in RIP signaling (*1*). Although, like γ-cleavage, ε-cleavage also exhibits diversity (*7*−*9*), the details of this diversity and the characteristics of the cleavage remain to be clarified. Both ε- and γ-cleavages are mediated by PS/γ-secretase (*2*), but whether the processes that determine the variety and the precision of these cleavages are common remains controversial. For example, it has been shown that ε-cleavage sites are associated with γ-cleavage sites (*7*, *15*, *16*); however, mutagenesis studies show that ε- and γ-cleavages are mediated by a distinct process (*17*).

PS is the proteolytic active center in the PS/γ-secretase protein complex (*2*, *18*). To exert its proteolytic function, PS must form a complex with at least nicastrin (*19*), PEN-2 (*20*), and APH-1 (*2*, *20*). Other factors that physiologically affect proteolysis, including the precision of cleavage, have not yet been identified. In contrast to other subcellular locations, AD-associated Aβ42 is produced in the ER without concomitant production of Aβ40. However, since this is not mediated by PS (*21*, *22*), whether the precision of PS-dependent proteolysis changes within cells depending on location or conditions remains unresolved.

In this study, using a cell-free γ-secretase assay, we examined whether the precision of cleavage by PS/γ-secretase is affected by its subcellular location. We demonstrate that, unlike γ-cleavage, ε-cleavage precision can drastically change depending on subcellular location and the pH. Relative cleavage at the ε51 site is more prone to occur on endosomes than on plasma membrane (PM) and at lower pH. In contrast, relative cleavage at the ε49 site is more likely to occur on PM than on endosomes and at higher pH. These results suggest that PS-dependent γ-secretase on plasma membrane and endosomes is functionally distinct.

MATERIALS AND METHODS

Antibodies. Rabbit antiserum 6618 was raised against a synthetic peptide KMQQNGYENPTYKFFEQMQN, which corresponds to the C-terminus of βAPP according to the methods described (*23*). The following antibodies were purchased from commercial sources: anti-Aβ antibody 4G8 (Senetec PLC), anti-Na−K ATPase (Upstate Biotechnology), anti-early endosome antigen 1 (BD Transduction Laboratories), anti-nicastrin (Sigma-Aldrich), anti-GM130 (BD Transduction Laboratories), and anti-tubulin (Santa Cruz Biotechnology). Also, antibody 12CA5 (Roche Diagnostics Inc.) was used to detect the N-terminal hemagglutinin-tagged dynamin-1 (Dyn-1) K44A mutant.

Cell Culture and cDNA Construct. Human embryonic kidney 293 (K293) cells stably expressing wild-type βAPP, wild-type PS1/βAPP Swedish (sw) mutant (*24*), or PS1 D385N/βAPP sw (*25*) were described previously. HeLa cells expressing Dyn-1 K44A under control of a tetracycline transactivator were kindly provided by Dr. Sandra L. Schmid (Scripps Institute, La Jolla, CA) (*26*). HeLa cells stably expressing βAPP sw were cultured without tetracycline (Sigma-Aldrich) for 48 h to induce expression of Dyn-1 K44A.

Membrane Fractionation and Cell-Free γ-Secretase Assay. The collected cells were homogenized with a Teflon homogenizer (20 strokes) in homogenization buffer (0.25 M sucrose and 10 mM HEPES, pH 7.4) containing a protease inhibitor cocktail (Roche) (*27*). The homogenate was centrifuged at 1000*g* for 5 min to remove nuclei and cell debris, followed by further centrifugation of the supernatant fraction at 100000*g* for 1 h. Following a single wash with homogenization buffer, the resulting precipitate was collected as the CMF and frozen in liquid nitrogen. Upon use, the frozen CMF samples were resuspended and immediately incubated in the reaction buffer [150 mM sodium citrate buffer (pH 5.0−7.4) containing 5 mM 1,10-phenanthroline (Sigma-Aldrich) and a 4× concentration of protease inhibitor cocktail (Roche)] for 20 min at 37 °C (cell-free incubation) (*28*, *29*). The reaction was terminated by placing the samples on ice.

Subcellular Fractionation. Linear gradients of 2.5−25% iodixanol (Optiprep; AXIS-SHIELD) were prepared. Postnuclear supernatant fractions from 24 dishes (ϕ = 14 cm) were loaded on the top of the gradient, followed by centrifugation for 3 h at 130000*g*. Each fraction was diluted with three volumes of homogenization buffer and centrifuged for 1 h at 100000*g* to precipitate the membranes. The precipitated membrane was used in cell-free γ-secretase assays or in immunoblots for marker proteins.

Metabolic Labeling. Following methionine starvation for 40 min, cells were metabolically labeled with 400 μCi of [^{35}S]methionine (Redivue Promix; Amersham Pharmacia Biotech) in methionine-free MEM for 20 min and chased for 30 min in DMEM containing 10% FBS and excess unlabeled methionine.

Immunoprecipitation/Autoradiography Analysis. Metabolically labeled CMF was lysed in RIPA buffer (1% Triton X-100, 0.5% sodium deoxycholate, and 0.1% SDS) containing a protease inhibitor mix (Sigma-Aldrich). The cell lysates were centrifuged at 10000*g* for 15 min, and the supernatant fractions were immunoprecipitated with 6618 antiserum for the detection of the C-terminal stub and de novo AICD. Following 10−20% Tris−tricine SDS−PAGE (Invitrogen), the gels were dried and analyzed by autoradiography (*3*).

Immunoprecipitation/Mass Spectroscopy (IP-MS) Analysis. IP-MS analysis was carried out as described previously (*3*). Following cell-free incubation, the CMF was sonicated four times for 10 s and then centrifuged at 100000*g* for 1 h. The supernatant were immunoprecipitated for 4 h at 4 °C in IP-MS buffer [140 mM NaCl, 0.1% *n*-octyl glucoside, 10 mM Tris-HCl (pH 8.0), 5 mM EDTA, and a protease inhibitor mix (Sigma-Aldrich)]. The heights of the MS peaks and molecular weights were calibrated using ubiquitin and/or bovine insulin β-chain as standards (Sigma-Aldrich). The relative peak heights were semiquantitatively analyzed (see Figure 3 in Supporting Information).

Immunoprecipitation/Immunoblot Analysis. Following cell-free incubation, the fractions were immunoprecipitated for 10 h at 4 °C in IP-MS buffer. After SDS−PAGE, the separated proteins were transferred to a PVDF or nitrocellulose (for detection of Aβ) membrane and probed with the indicated antibodies (*30*). The nitrocellulose membrane was heated for 10 min in boiling PBS before blocking. AICD and Aβ levels were semiquantified by chemiluminescence using an LAS3000 scanner and Multi Gauge Ver3.0 software (Fujifilm).

Transferrin Uptake Assay. To determine the level of internalized transferrin, the treated cells were washed three times in Hank's balanced salt solution (Sigma-Aldrich), pH 7.4, and then treated for 7 min at 37 °C with 8 μg/mL biotin−